Carlson, K.D., Ou, S., and Beckermann, C., "Feeding and Risering of High Alloy Steel Castings," in Proceedings of the 57th SFSA Technical and Operating Conference, Paper No. 4.5, Steel Founders' Society of America, Chicago, IL, 2003.

Feeding and Risering of High Alloy Steel Castings

Kent D. Carlson, Shouzhu Ou and Christoph Beckermann[1]

Department of Mechanical and Industrial Engineering

The University of Iowa, Iowa City, IA 52242

ABSTRACT

A more accurate, less conservative set of feeding distance and riser sizing rules is developed for high alloy steel grades CF-8M, CA-15, HH, HK and HP. These rules are designed to produce radiographically sound castings at 2 pct sensitivity. By comparing results between plate casting trials and the corresponding simulations of those trials, a relationship is shown to exist between a local thermal parameter known as the Niyama criterion and ASTM shrinkage x-ray level. This relationship was then used in an extensive set of casting simulations to numerically determine feeding distances for a wide range of casting conditions. It is shown that the feeding distance rule developed in an analogous earlier study for carbon and low alloy (C&LA) steels can also be used for these high alloy grades, provided that the feeding distance is modified by a multiplier that accounts for the high alloy steel grade. In addition, it is shown that multipliers for superheat, sand mold material and the use of chills developed in the earlier work are also valid with these high alloy steel grades. In comparison with previously published high alloy feeding distance rules, the present rules are shown to provide longer feeding distances in most casting situations. This study also investigates riser sizing rules. It is determined that for open top risers, the previously published C&LA riser sizing rule is also valid for high alloy steels. This rule is less conservative than existing high alloy riser sizing rules. In addition, for vented blind top risers, it is shown that the previously published rules are overly conservative.

[1] Author to whom correspondence should be addressed. Telephone: (319) 335-5681, FAX: (319) 335-5669, E-mail: becker@engineering.uiowa.edu

1 INTRODUCTION

In a time when competition for business in the steel casting industry is very intense, it is of utmost importance for foundries to produce high-quality castings at the lowest possible cost. Not only is there competition for business between steel foundries, but the foundries must also compete with businesses that produce steel products by other techniques (e.g., forging or fabricating), as well as with businesses that produce products from materials other than steel (e.g., aluminum). As such, the savings brought about by a relatively small increase in casting yield may well determine whether a foundry succeeds or fails in its competition to produce a particular part. An increase in casting yield will decrease the cost of castings due to decreased production costs; with increased yield, production of the same number of castings requires less melted metal and fewer heats, as well as reduced labor and materials costs required for production. Also, higher yield usually has the side benefit of lower casting cleaning costs. One effective way to improve casting yield is through riser optimization, where "optimized" means (1) the riser has the minimum possible volume to provide sufficient feed metal to the casting, without the riser pipe extending into the casting; and (2) the smallest number of risers are utilized, while still ensuring that the risers are close enough to each other to produce a sufficiently sound casting.

Computer simulation of the casting process is becoming an indispensable tool in the effort to achieve increased casting yield. Through the use of simulation, foundries are able to evaluate modifications to casting designs without having to actually produce the casting, thus saving time, material resources and manpower. However, computer simulation must be applied on a case-by-case basis, and its effective use requires expertise as well as accurate data for many process variables. Due to these limitations, risering rules are still widely used in the steel casting industry. Risering rules dictate riser size and placement by determining (1) the riser size necessary to supply adequate feed metal to a casting section, and (2) the feeding distance, which is the maximum distance over which a riser can supply feed metal to produce a sound casting. A recent survey indicates that simulation is used for less than ten percent of the tonnage of steel castings produced, and that risering rules (or rules-based software) are used to rig about eighty percent of the tonnage produced.[1,2] Due to the prevalence of rules-based rigging in the steel casting industry, any attempt to increase casting yield in a general sense must begin with these rules. Even if simulation is used, risering rules are still useful to develop a reasonable starting point for simulation, which will shorten the iterative optimization cycle.

A great deal of effort has been expended to develop rules for determining riser feeding distances in steel castings. Many researchers have developed empirical relations for determining feeding distances in carbon and low-alloy (C&LA) steels. These rules are typically based on experimental casting trials performed in the 1950's by Bishop, Myskowski and Pellini at the Naval Research Laboratory (NRL),[3-7] as well as on similar casting trials conducted by the Steel Founders' Society of America (SFSA).[8] An extensive review of empirical feeding distance relations for C&LA steels is provided in previous work by the current authors.[9,10] Numerical determination of feeding distances for C&LA steels has also been investigated. One of the earliest efforts was undertaken at Case Western Reserve University (Cleveland, OH) by Spiegelberg,[11,12] Maier[13] and Ghun,[14] under the direction of Professor J.F. Wallace. The idea of this work was that the solidification gradient could be used to determine whether or not shrinkage porosity would form in a casting. Spiegelberg theorized that if the solidification gradient near the end of solidification dropped below some minimum value, shrinkage porosity would form. They determined the minimum value by comparing their numerical results to the NRL casting trial results.[3-7] More recently, the present authors[9] developed a methodology to numerically determine feeding distances in low-alloy steel castings through the use of the Niyama criterion,[15] which is a local thermal parameter defined as $G/\sqrt{\dot{T}}$, where G is the temperature gradient and $\dot{T}$ is the cooling rate. By comparing radiographic testing (RT) casting soundness results from an extensive set of plate casting trials with Niyama criterion values computed from simulations corresponding to each casting trial, a correlation was found between casting soundness and the minimum Niyama criterion value. It was determined that, if the minimum Niyama value of a casting section is greater than 0.1 $K^{1/2}s^{1/2}mm^{-1}$, the section will be radiographically sound (i.e., no shrinkage visible on x-ray). Further, if a section is unsound, shrinkage is likely to occur in regions where the Niyama criterion for that casting section is below the threshold value.

To the authors' knowledge, the only extensive research effort to develop feeding distance rules specifically for high alloy steels was performed by Varga, Stone and Lownie[16-19] at Battelle Memorial Institute, under a grant from the Alloy Casting Institute (ACI). Varga *et al*. began with the shape factor concept first proposed by Bishop *et al*.;[3-7] the shape factor of a casting section is calculated from the section's length, width and thickness according to the relation: $SF = (L + W)/T$. Varga *et al*. developed empirical charts that gave the appropriate riser size and feeding distance for a given shape factor, assuming the riser was centrally located on the casting section. This was initially done for the C&LA castings produced at the Naval Research Laboratory,[3-7] to determine if the methodology provided feeding distances and riser sizes that agreed with those of Bishop *et al*. The results were encouraging, so Varga *et al*. proceeded to perform high alloy casting trials. They cast plates in sixteen foundries, in CF-8, CA-15, HH, HF and HT alloy grades (including multiple compositions of several grades). Top-risered plates were cast with thicknesses T = 1.27, 2.54 and 5.08 cm (0.5, 1 and 2 in.), with an emphasis on T = 1.27 and 2.54 cm (0.5 and 1 in.), because those values are more common in the high alloy casting industry. The width-to-thickness ratios (W/T) used for top-risered plates ranged from 1 to 10. Side-risered plates were only cast with thickness T = 2.54 cm (1 in.), with W/T ranging from 1 to 5. All plates (top- and side-risered) were cast with blind risers, both with and without cracker cores. Feeding distances were determined by finding the maximum length that a riser could feed to produce a sound casting, where soundness was defined as no visible shrinkage on radiographs filmed at 1.5 pct sensitivity. The end result of this work is three empirical feeding distance charts: one for blind top risers feeding 1.27 cm (0.5 in.) thick sections, one for blind top risers feeding 2.54 cm (1 in.) thick sections, and one for blind side risers feeding 2.54 cm (1 in.) thick sections. An important note regarding these high-alloy feeding distance charts is that the feeding distance is defined from the center of the riser to the edge of the casting, rather than from the edge of the riser to the edge of the casting, as in the C&LA rules (see Figure 1). These inconsistent definitions make direct comparison of C&LA and high alloy feeding distances difficult.

Considerable research has also been done to develop riser sizing guidelines for steel castings. Early quantitative approaches developed by Chvorinov[20] and Janco[21] allowed a foundry engineer to determine the riser size necessary to ensure that the riser would solidify after the casting section it was feeding. These methods were based on the work of Chvorinov,[22] who found that solidification time was directly related to a casting's volume-to-surface-area ratio. While these methods provided a riser that solidified after the casting, they did not ensure that the casting would be free from under-riser shrinkage. Wlodawer[23] termed Chvorinov's volume-to-surface-area ratio the "solidification modulus," and developed the modulus method. According to his method, if the modulus of the riser is 20% larger than the modulus of the casting section to be fed, the riser will be sufficient and free from under-riser shrinkage. The modulus method is valid for both C&LA and high alloy steels, primarily because it employs a significant factor of safety. Ruddle[24] modified Wlodawer's method by explicitly accounting for the volumetric shrinkage of the casting section, which reduces the factor of safety somewhat to provide a more optimized riser size.

Caine[25] developed a riser sizing method for C&LA steels that also ensures castings free of under-riser shrinkage, by determining adequate riser size from an empirical relationship between the riser-volume-to-casting-volume ratio and a "freezing ratio," which is the surface-area-to-volume ratio of the casting divided by that of the riser. A disadvantage to this method is that it requires trial-and-error; one simply guesses a riser size, performs the calculations, and checks whether or not the size selected is adequate. If not, a larger size is chosen, and the calculations are repeated. This disadvantage was overcome in a method proposed by Bishop, Myskowski and Pellini,[26] who developed a direct method for determining riser size in C&LA steels. They replaced Caine's freezing ratio with a shape factor for the casting section to be fed (as discussed above, $SF = (L + W)/T$). Once the shape factor for a casting section is calculated, the riser size can be directly determined through an empirical relation. They developed this empirical relation for riser height-to-diameter ratios from 0.5 to 1, and stated that a ratio larger than one decreases yield without providing additional benefits, while a ratio smaller than 0.5 produces a riser with a relatively large diameter that requires excessive cleaning costs to remove. They also provided a method to modify the riser size for complex-shaped castings (i.e., casting sections with appendages).

As was the case for high alloy feeding distance rules, the only extensive effort to develop riser sizing rules for high alloy steels is the work of Varga *et al*.[16-19] In their casting trials, they used blind risers (top and side) that had height-to-diameter ratios of one. They used the shape factor concept of Bishop *et al*.,[26] but Varga *et al*. determined the sufficient/minimum riser volume (and hence diameter and height, since $H/D = 1$) in a somewhat different manner than did Bishop *et al*. After determining the appropriate riser sizes for all the experimental castings, Varga *et al*. developed relations to directly determine riser sizes for blind top and blind side risers, based on the shape factor of the section to be fed. As with their feeding distance rules, these riser sizing rules were developed for high alloy grades CF-8, CA-15, HH, HF and HT. Analogous to the work of Bishop *et al*., they also provided a method to modify the riser size for complex-shaped high alloy casting sections. For several reasons, the riser sizing methodology of Varga *et al*. is more conservative than that of Bishop *et al*.; this will be discussed in further detail in the section that describes the new high alloy riser sizing rules.

As a final note on riser sizing rules, some numerical research has been performed on riser size optimization. Morthland *et al*.[27] developed a scheme to iteratively perform entire solidification simulations and optimize the riser size based on the resulting riser pipes. Ou[28] developed a mathematical riser model that simulated riser pipe formation based on liquid and solidification shrinkage coupled with fluid dynamics, and then optimized riser size through the minimization of a cost function that provided the minimum riser size while ensuring the riser pipe did not penetrate beyond the riser into the casting. Both of these numerical methods, which are applicable to both C&LA and high alloy steels, produced riser pipes that were in good agreement with actual castings.

In 1973, the SFSA compiled the available low alloy feeding distance rules (the results from the NRL[3-7] and SFSA[8] casting trials, and the numerical predictions performed at Case Western Reserve University[11-14]), the low alloy riser sizing rules of Bishop *et al*.,[26] and the high alloy feeding distance and riser sizing rules developed by Varga *et al*.[16-19] into a handbook entitled *Risering Steel Castings*.[29] The data in this handbook, presented as charts, nomographs, equations, and procedures for risering steel castings, is intended to assist foundry engineers in the placement and sizing of risers on steel castings. Although this handbook is thirty years old, it is still used in foundry practice today. However, there has been substantial feedback from SFSA member foundries indicating that the risering rules contained in *Risering Steel Castings*, while adequate, are often overly conservative.[1] Also, it was noted that these rules do not account for differences in sand mold material, alloy composition (for low alloy steels), or superheat, all of which are known to affect the distance over which a riser can provide feed metal to a casting section. For high alloy steels, superheat is particularly important, as foundries typically use significantly larger superheats for high alloy steels than for low alloy steels.

To address the need for more accurate, less conservative risering rules, the present authors recently developed a new set of C&LA feeding distance rules.[9,10] As discussed earlier in this section, through extensive casting trials and corresponding simulations of each trial casting, a correlation was developed between the Niyama criterion and radiographic soundness. Once this correlation was established, a large number of simulations were performed in order to determine feeding distances for a wide variety of casting conditions. Based on the resulting information, a new set of feeding distance rules was designed to produce radiographically sound castings at 2 pct sensitivity. Rules are provided for end-effect feeding distance and lateral feeding distance for top risers, as well as feeding distance for side risers. In addition, multipliers are provided to apply these rules with end chills and drag chills, as well as to tailor these rules to different steel alloy compositions, sand mold materials and pouring superheats. These new rules are shown to provide longer feeding distances in most casting situations. The C&LA riser sizing methodology of Bishop *et al*.[26] was not revised, because it was found to be adequate (i.e., not overly conservative). These rules were also published in an SFSA report[30] that was distributed among SFSA member foundries.

The objective of the present study is to develop a new, less conservative set of riser feeding distance rules for common high alloy steel grades. The approach taken will be completely analogous to the present authors' C&LA feeding distance rule development just discussed. High alloy casting trials will be coupled with simulation to develop the necessary correlation to develop high alloy feeding distance rules. In addition, high alloy riser sizing rules are examined; based on this investigation, less conservative riser sizing rules are suggested. The use of these new high alloy rules will provide less conservative riser sizes and feeding distances in most instances, which will increase high alloy casting yield.

2 FEEDING DISTANCE TERMINOLOGY

Before discussing the development of the feeding distance rules, it is prudent to carefully define the terms that will be used for this development. The feeding distance (*FD*) is defined as the maximum distance over which the riser can provide feed metal *resulting in a radiographically sound casting*. In the case of the SFSA guidelines for high alloy steels, *FD* is defined from the center of the riser to the edge of the casting section (see FD_{HA} in Figure 1), and soundness is defined as Class I soundness at 1.5 pct radiographic sensitivity.[29] Class I soundness implies that some shrinkage is allowable, provided it is less severe than in the Class I standard radiographs. For the present study, *FD* is defined from the edge of the riser to the furthest point in the casting section (see *FD* in Figure 1), and soundness is defined as radiographically sound at 2 pct sensitivity (i.e., no shrinkage visible on x-ray). Another way to explain how the feeding distance is measured in the present study is to draw a circle centered about the riser with a radius equal to the feeding distance plus the riser radius (see Figure 1). Then the casting section inside the circle is fed by that riser. For multi-risered castings (such as in lateral feeding), the circles must overlap such that all sections of a casting are inside these circles. It is noteworthy that this definition of *FD* is the same as the one used by the present authors in the C&LA feeding distance rule development;[9,10,30] the importance of this consistency will become evident when the high alloy feeding distance rules are developed.

A similar term that will be commonly used in this work is feeding length (*FL*). The feeding length of a casting section is simply the distance from the riser to the furthest point in the section. It is the length to be fed. It is purely geometrical, and *implies nothing about the soundness of the casting section being fed*. If the feeding length is less than or equal to the feeding distance, the casting section will be sound; if the feeding length exceeds the feeding distance, the casting section is likely to have visible shrinkage porosity.

There are two other terms that are important to understand when considering feeding distances: riser zone and end zone. Since the riser remains hotter than the casting section to be fed, it provides a temperature gradient that facilitates feeding. The length over which this riser effect acts to prevent shrinkage porosity is called the riser zone length (*RZL*), which is measured radially outward from a riser. This is illustrated for a top riser in Figure 2. The cooling effect of the mold at the end of a casting section also provides a temperature gradient along the length of the casting section to be fed. This is called the end effect, and it produces a sound casting over the so-called end zone length (*EZL*), which is measured normal to the end of a casting section. This is depicted in Figure 3. The feeding distance, *FD*, is a function of *RZL* and *EZL*. As an example, consider Figure 4. For the casting section in this figure to be sound, the entire section must be within a riser zone or end zone region (note that end zones extend from the top and bottom edges (EZL_2) of this casting, as well as from the right edge (EZL_1)). In the case shown in Figure 4 ($W > 2EZL_2$), the feeding distance is determined by the largest casting section that can still be completely covered by riser zones and end zones (Figure 4a). If the size of the casting section to be fed increases beyond that shown in Figure 4a, the feeding length of this larger casting section will exceed the feeding distance, and shrinkage porosity will form in the portions of the casting not covered by a riser zone or end zone, as shown in Figure 4b. Note that if $W \leq 2EZL_2$, or if there are multiple risers, the end zone/riser zone requirements for a sound casting change somewhat. This is discussed in detail in the earlier C&LA work[9,30]

3 HIGH ALLOY PLATE CASTING TRIALS

As part of the present study, four different foundries cast a total of 165 high alloy plates with a single top riser. The alloys cast were CF-8M (125 plates), HH (20 plates) and HP (20 plates). The original intent was to also cast plates from CA-15 and HK, but the foundries that had agreed to perform those trials had to withdraw from the project. It will be shown in the next section, however, that it was possible to develop rules for these alloys without performing their casting trials. The general casting configurations used for high alloy plate trials are shown in Figure 5; one set of plates (25 CF-8M plates) was cast vertically (Figure 5b), and the rest horizontally (Figure 5a). Again, recall that the feeding lengths *FL* shown in Figure 5 are purely geometrical, and imply nothing about casting soundness. The casting trial plates can be categorized into four groups, based on their cross-section: 20 of the plates had a cross-section 1.27 cm thick by 2.54 cm wide (0.5 in. *T* by 1 in. *W*), 50 plates were 2.54 cm thick by 14.0 cm wide (1 in. *T* by 5.5 in. *W*), 70 plates were 2.54 cm by 20.3 cm (1 in. *T* by 8 in. *W*), and the remaining 20 plates were 1.27 cm by 15.2 cm (0.5 in. *T* by 6 in. *W*). For brevity, these groups of plates will hereafter be referred to by their width-to-thickness (W/T) ratios: W/T = 2, 5.5, 8 and 12, respectively. The W/T = 5.5 and 8 plates were designed with riser diameters D_R = 10.2 cm (4 in.), the W/T = 12 plates used D_R = 15.2 cm (6 in.), and the W/T = 2 plates used D_R = 3.8 cm (1.5 in.). The riser height-to-diameter ratios were all designed to be unity (H_R/D_R = 1); this was approximately achieved in practice, except for the W/T = 2 and W/T = 12 plates, where the casting foundry decided to use H_R/D_R ratios of 4.67 and 3, respectively. Several different lengths (*L*) were cast for each of these groups of plates, with the lengths selected to produce plates ranging from radiographically sound to ASTM shrinkage x-ray level 5 (very unsound). All of the plates described above were cast in either PUNB (furan) or green sand molds. The casting trial data are summarized in Table 1.

When conducting the casting trials, it was envisioned that the trials would include the normal variations in casting conditions that are possible in foundry practice. These variations would then be considered in the analysis of the results. Therefore, detailed information was collected on the casting process for the trial plates, and all information was recorded in detailed data sheets that were filled out by the participating foundries. The casting parameters that were recorded were: pouring temperature, pouring time, steel chemistry, mold material, actual casting rigging and mold-box geometry. In addition, each plate cast in these trials was examined by radiographic testing (RT) according to ASTM E94[31] procedures, using E446[32] reference radiographs (for casting sections up to 5.08 cm (2 in.) thick]. Based on this examination, an ASTM shrinkage RT level was assigned to each plate.

The results of the casting trials are given in Figures 6 through 9, which plot the feeding lengths of the W/T = 2, 12, 5.5 and 8 plates, respectively, against the resulting ASTM shrinkage x-ray level for each corresponding plate. The different hollow symbols indicate plates cast by different foundries. When a number appears next to a symbol (or group of overlapping symbols), this indicates the number of plates of that feeding length with the same x-ray level. The shrinkage x-ray levels in these figures range from 0 to 5, where level 0 indicates that the plate was radiographically sound (i.e., absolutely no indications visible on x-ray). While level 0 is not a standard ASTM x-ray level, it is used in this study because it provides additional information. Also shown in these figures are the mean x-ray levels for each value of *FL*, as well as error bars indicating one standard deviation. The mean values and error bars are not intended to provide meaningful statistical data—the number of plates at each feeding length is generally small, and x-ray levels are quantized rather than continuous data—rather, they are provided to more clearly indicate the trends in the data.

Figures 6 and 7 show the results for the 1.27 cm (0.5 in.) thick plates. Some plate lengths were chosen for both of these sets of plates that are well in excess of the existing high alloy feeding distance rules for 1.27 cm (0.5 in) plates, in an attempt to produce unsound plates with x-ray levels between 1 and 5. However, all the plates represented in Figures 6 and 7 have shrinkage levels of 0 or 1. The sound radiographic results of these casting trials are not entirely surprising; it is known that, for thin casting sections (i.e., less than 2.54 cm (1 in.) thick), the feeding distance becomes highly dependent on the filling process.[29] If a thin section is gated through the riser, feeding distances substantially longer than those predicted with rules for thicker sections can be achieved.[3] This phenomenon can be understood through casting simulation (using the methodology to determine feeding distance, riser zone length and end zone length described in Section 5). Gating through the riser enhances feeding distance by increasing the riser zone length; it has little effect on the end zone length. This increase in riser zone length is moderate for castings that have thickness 2.54 cm (1 in.) or larger, but becomes considerable when the thickness decreases to 1.27 cm (0.5 in.).

Figures 8 and 9 show the results for the 2.54 cm (1 in.) thick plates. Notice that, as plate length increases, the average shrinkage x-ray level tends to increase as well. An interesting feature of the casting trial results visible in these figures is the spread of x-ray levels for a given feeding length. Notice that there are several instances in Figures 8 and 9 where the range of x-ray levels at a given feeding length varies by three to five levels. This is particularly evident in Figure 9. This scatter is partially due to the variability in the casting process. Steel composition, pouring temperature, pouring time, mold material, etc. varied from foundry to foundry. The effect of such differences in the production setting is visible in the results shown in Figures 8 and 9; notice that the variation in x-ray level at a given feeding length for a given alloy cast by one foundry is generally smaller than the total variation at that feeding length. Some casting parameters (e.g., pouring temperature) even varied to some degree within a single foundry. Another factor contributing to the scatter in x-ray level at a given feeding length is the variability inherent in assigning x-ray levels to a given radiograph (about ±1.4 x-ray levels, on average[33]). A final cause of the scatter is the presence of gas porosity (of a spherical nature, and thus not considered in the shrinkage rating) in some of these plates.

4 SIMULATION OF CASTING TRIALS

Based on the information given on the casting trial data sheets for the plates, simulations were performed for each plate for which unique casting data was available, using the commercial simulation software package MAGMASOFT.[2] By using this detailed casting information as input for the simulations, it was possible to account for the variability due to differences in

[2] Although MAGMASOFT[34] was used in this work to simulate the casting trials, a number of simulation packages are available, and most of them are capable of calculating the Niyama criterion. In fact, the authors performed a comparison between MAGMASOFT and AFSolid,[35] and determined that the Niyama values calculated by these two packages for the same casting conditions are similar, provided that one takes care to ensure the Niyama values are calculated in the same manner (e.g., evaluated at the same temperature), and that the values are converted to the same units.[36]

casting parameters from foundry to foundry (and from plate to plate). Simulation of the filling process was included, to model the flow of the melt through the gating and into the castings, as well as the cooling of the metal that occurs during this process. The thermophysical properties of each steel alloy considered were computed using the interdendritic solidification computer software (IDS) developed by Miettinen et al.[37,38] The solid fraction versus temperature and density versus temperature curves for the alloys of interest are shown in Figure 10. Also included in this figure are the corresponding curves for a plain carbon steel (AISI 1025), for comparison. Three different CF-8M compositions were computed (with 0.03, 0.06 and 0.08 pct carbon), to correspond with the different compositions cast by the foundries involved. In Figure 10a, note the similarity in the freezing ranges for these alloys; the curves shift to the left (to lower temperature ranges) as the amount of alloying elements increases, but the sizes are generally similar. However, Figure 10b shows that there are greater differences among these alloys in their density change during solidification (i.e., solidification shrinkage). These differences in shrinkage contraction will be discussed in the riser sizing section.

Figure 10 can be used to explain the rationale behind developing feeding distance rules for HK and CA-15 alloys without performing those casting trials. The composition of HK is very similar to that of HH and HP, differing primarily in the nickel content. Fortunately, the nickel content of HK is between that of HH and HP. Thus, one would expect the thermophysical properties of HK to be similar to those of HH and HP. This is evident in Figure 10a, where the solidification path of HK44 is seen to fall between HH and HP. Figure 10b shows that the density curves for these three alloys are very similar as well. Similarly, the composition of CA-15 falls between plain carbon steel and CF-8M. Figure 10 shows that both the solidification path and density curves of CA-15 fall between plain carbon steel and CF-8M values. Because the properties of HK and CA-15 lie between those of alloys that were cast in the casting trials (plain carbon steel plates were cast in the low-alloy casting trials[9]), and because the primary purpose of the casting trials was to validate the simulation results used to develop the feeding distance rules, it was deemed acceptable to develop feeding distance rules for HK and CA-15 based on simulation alone.

The simulations of the plate casting trials provided the distribution of the Niyama criterion throughout the castings. An example of the Niyama-value distribution in a typical plate is shown in Figure 11. This is a simulation of a 2.54 by 20.3 by 43.2 cm (1 by 8 by 17 in.) HH plate, which is long enough to exceed the feeding distance for the riser (see the results for FL = 34.4 cm (13.5 in.) in Figure 9). In the casting trials, centerline shrinkage was commonly found in plates with these dimensions. Notice that, in both the top view (Figure 11a) and side view (Figure 11b) cross-sections, the lowest Niyama values (i.e., the darkest cells) are confined to the center of the plate. The region with the lowest Niyama values corresponds very closely to the region where centerline shrinkage occurs.

For each simulated plate, the minimum value of the Niyama criterion in the central-thickness cross-section (i.e., the plane one would see in a typical x-ray of the plate, Figure 7a) was determined. In addition, the total area in that same cross-section with Niyama criterion values below some critical value was also recorded for each simulation. It is important to note that care must be taken when extracting Niyama values from simulation results. For example, in the present study, it was necessary to turn off the postprocessor's interpolation function (which is set "on" by default in MAGMASOFT) in order to determine the correct Niyama values for each metal cell of interest. Figure 12 plots the minimum Niyama values of the *W/T* = 8 plates against the feeding length of each plate. There is a very obvious trend of decreasing minimum Niyama values as the feeding length increases (and hence plate soundness decreases). Analogous plots for the *W/T* = 2, 5.5 and 12 plates look very similar to Figure 12; for this reason, they are not presented here.

Computational results such as those in Figure 12 can be combined with the experimental results shown in Figures 6 through 9 by eliminating the feeding length from these figures and simply plotting the ASTM shrinkage x-ray level determined for each plate versus the minimum Niyama value resulting from the simulation of that plate. In other words, one can plot the measured soundness, in terms of shrinkage x-ray level, against the predicted soundness, in terms of minimum Niyama value. This is shown in Figure 13, which includes all 165 high alloy plates (*W/T* = 2, 5.5, 8 and 12) described in the previous section. The first noteworthy feature of this figure is a definite tendency toward lower and lower minimum Niyama values as the x-ray level increases. This trend is highlighted in the plot inset in the upper-right corner of Figure 13, which shows the mean value of Ny_{min} for plates having x-ray levels from level 1 to level 4. The mean values for each x-ray level are shown with bars indicating the size of the range from minus one to plus one standard deviation from the mean. This is an indication of the scatter of the values for plates with a given x-ray level. No mean minimum Niyama values are given for level 0 or level 5 because the mean value for level 5 plates could be made almost arbitrarily small by casting a large number of very long plates, and the mean value for level 0 plates could similarly be made almost arbitrarily large by casting a large number of short plates. Note that the minimum Niyama value asymptotes to zero as the x-ray level increases to level 5, and that the scatter in Ny_{min} tends to decrease as the x-ray level increases.

It is also apparent from Figure 13 that a plate with a relatively large value of Ny_{min} will have a low x-ray level. Note that all of the plates with a minimum Niyama value greater than 0.2 are level 1 or better, and almost all of the plates with $Ny_{\mathrm{min}} > 0.1$ are level 1 or better. The two plates with $Ny_{\mathrm{min}} > 0.1$ that have x-ray levels higher than level 1 are considered outliers; they are the result of (1) the previously mentioned scatter in the experimental data that could not be accounted for in the simulations, and (2) differences between the actual casting conditions and the values that were recorded. As an example of the latter, if the recorded superheat was higher than the actual superheat, the simulation would result in a plate more sound (hence, with a larger Ny_{min}) than was produced in the trials. It is evident that there is a transition, as the Niyama value decreases down to somewhere around 0.1 to 0.2, from radiographically sound plates to unsound plates. For the present study, it was desirable to define some threshold value to denote this transition. The value chosen as the threshold is $Ny_{\mathrm{min}} = 0.1\ \mathrm{K}^{1/2}\mathrm{s}^{1/2}\mathrm{mm}^{-1}$. This is the same threshold value that was chosen for the C&LA feeding distance rules developed by the present authors[9]; a thorough justification of the choice is provided in this earlier work.

While it is true that a relatively large Niyama value indicates that a plate will probably have a low x-ray level, the converse is not true: a small value of Ny_{min} does not necessarily imply that the corresponding plate will have a high x-ray level. This is evident from the large number of plates in the lower-left corner of Figure 13 that are level 1 or better, and yet have $Ny_{\mathrm{min}} < 0.05$. Although this may appear troubling at first glance, it can be explained by considering Figure 13 in conjunction with Figure 14, which plots the shrinkage x-ray level of the *W/T* = 5.5 plates against the area of these plates with Niyama criterion values below the threshold value of 0.1, measured from the corresponding plate simulations (see Figure 11a). Figure 14 includes the values for each individual plate (numbers next to symbols indicate multiple plates with the same value), as well as the mean area for all of the plates at each x-ray level plus/minus one standard deviation. As in Figure 13, no mean values are given for level 0 or level 5 in these figures, because the mean areas for these levels are rather arbitrary. An area of zero indicates that the minimum Niyama value is greater than 0.1. Figure 14 shows that, as the x-ray level of a plate increases, the area with Niyama values less than 0.1 tends to increase as well. The standard deviation bars show that there is a significant amount of scatter in this data, however. From Figure 14, it can be seen that the level 0 and level 1 plates in Figure 13 with $Ny_{\min} < 0.1$ generally have very small areas with Niyama values less than 0.1. Thus, a small minimum Niyama value does not necessarily imply that the plate should have a high x-ray level; if the area with $Ny < 0.1$ is small, the plate may still be radiographically sound. The analogous plot for the *W/T* = 8 plates shows the same trends, and thus is not shown; the *W/T* = 2 and 12 plates all have x-ray levels of 0 or 1, so a plot of this type is not useful.

5 CALCULATION OF FEEDING DISTANCE

At this point, it is necessary to review the C&LA feeding distance rule development previously performed by the present authors.[9,10,30] The reason for this is that the high alloy rules will be shown to be directly linked to the previously developed rules for C&LA steels. As mentioned earlier, the high alloy rule development described in this paper was performed in a manner completely analogous to the development of the C&LA rules. Comparison between the C&LA casting trials and the simulations of those trials led to the same conclusion determined for high alloy steels in the previous section: if the minimum Niyama value in a casting section is greater than 0.1 $K^{1/2}s^{1/2}mm^{-1}$, the casting section should be radiographically sound. Once this relationship was established, a great number of casting simulations were performed. These simulations were run without considering filling; i.e., the simulation began with the mold cavity full of metal at T_{pour}. Simulating without filling results in slightly shorter feeding distances, which means that the rules developed here are slightly conservative; however, the overall effect is very small. Simulations were performed using values of plate thickness *T* ranging from 2.54 cm to 30.5 cm (1 in. to 12 in.). For each thickness, plates were simulated with widths corresponding to *W/T* ratios ranging from 1 to 17. For each value of *T* and *W/T*, the plate length *L* was varied until the minimum Niyama value in the central-thickness cross-section (i.e., typical x-ray plane) was equal to 0.1 $K^{1/2}s^{1/2}mm^{-1}$. An example illustrating this is provided in Figure 15. If the plate shown in this figure was made any longer, the minimum Niyama value would drop below 0.1, and radiographic soundness would no longer be expected. The plate length for which $Ny_{\min} = 0.1$ was used to determine the feeding distance (*FD*), as well as the riser zone length (*RZL*) and end zone length (*EZL*), as shown in Figure 15. The end effect (i.e., single top riser) feeding distance rule resulting from this C&LA work is shown in Figure 16, which gives the feeding distance as a function of *W/T*. By dividing *FD* by the thickness *T* (the dimension into the page for the casting sketch shown in Figure 16), it was possible to represent the feeding distance with a single curve for all section thicknesses in the range being considered. The curve in Figure 16 can be represented by the following polynomial expression:

$$\left(\frac{FD}{T}\right)_{\text{end effect}} = -4.29\times10^{-4}\left(\frac{W}{T}\right)^4 + 0.0174\left(\frac{W}{T}\right)^3 - 0.266\left(\frac{W}{T}\right)^2 + 1.99\left(\frac{W}{T}\right) + 1.97 \qquad (1)$$

Equation (1) is accurate up to $W/T = 15$, beyond which FD/T has a constant value of 9.0.

Figure 16 and Equation (1) represent the C&LA feeding distance rule for the base case casting conditions, which are:

- AISI 1025 steel,
- PUNB (furan) sand mold,
- 60°C (108°F) pouring superheat.

In addition to these base case casting conditions, rules were also developed for different sand mold materials, C&LA steel compositions, pouring superheats, and cooling conditions (end chill, drag chill). It was determined that variations from the base case could all be accounted for with simple multipliers. Then the feeding distance for casting conditions other than the base case conditions could be computed with the equation

$$\left(\frac{FD}{T}\right)_{\text{different conditions}} = \left(\frac{FD}{T}\right)_{\text{base case}} \times C_{\text{superheat}} \times C_{\text{cast alloy}} \times C_{\text{sand mold}} \times C_{\text{cooling conditions}} \qquad (2)$$

where $(FD/T)_{\text{base case}}$ represents the feeding distance determined from Figure 16 or Equation (1), and the multipliers in Equation (2) are provided in Table 2.

For the high alloy steel rule development, just as in C&LA steels, once the critical minimum Niyama value of 0.1 was determined, a large number of casting simulations were performed for each alloy under consideration (CF-8M, CA-15, HH, HK and HP). Plate thickness T was again varied from 2.54 cm to 30.5 cm (1 in. to 12 in.), and for each thickness, plates were simulated with widths corresponding to W/T = 1, 2, 4, 6, 8 and 12. As in the previous work, the plate length L was varied for each plate until the feeding distance, riser zone length and end zone length were determined (as in Figure 15). An example of the results of this effort is shown in Figure 17. This figure contains curves representing feeding distance, riser zone length and end zone length for CF-8M (0.06 pct carbon). All simulations represented in this figure were performed using furan sand, and a superheat of 100°C (180°F). Again, FD, EZL, RZL and W are all normalized by the thickness T, so that the feeding distance, riser zone length and end zone length can each be represented by a single curve for all section thicknesses in the range being considered. By comparing the CF-8M curves in Figure 17 to the CF-8M simulation results for the different thicknesses, one can see that the curves were generated using the average values at each W/T ratio for casting sections with thicknesses ranging from 2.54 to 30.5 cm (1 to 12 in.). Note that as thickness decreases, FD/T increases slightly. However, it is a relatively small change, and as such it is neglected for the sake of producing a single feeding distance curve for all values of thickness.

Also shown in Figure 17 is the feeding distance rule for 1025 steel under these casting conditions. Except for the superheat, the conditions for this curve are all the base case conditions (see Table 2). Therefore, this curve can be determined by multiplying the feeding distance given in Figure 16 or Equation (1) by the superheat multiplier for 100°C (180°F), which is $C_{superheat}$ = 1.08. Notice that this curve and the feeding distance rule for 0.06 pct carbon CF-8M are very similar. In fact, these rules differ by a scale factor; i.e., if the 1025 steel curve is scaled by the factor 0.978 (determined through regression analysis), the result is essentially coincident with the CF-8M curve in this figure. The correlation between these feeding distance curves is possible because the high alloy rules were developed in a manner completely consistent with the methodology used to develop the C&LA rules. Besides consistent methodology, two other important areas of consistency are worth noting: first, the definitions of feeding distance, riser zone length and end zone length used for the C&LA and high alloy rules are identical; and second, the same value of minimum Niyama criterion was chosen as the critical value for both C&LA and high alloy steels.

Further evidence of the scalability between C&LA and high alloy feeding distances is given in Figure 18, which shows the feeding distance results for CA-15, again with furan sand and 100°C (180°F) superheat. The open circles represent the average of the simulation results over all thickness values computed at each value of *W/T*. The upper curve again represents the feeding distance rule for AISI 1025 steel for these casting conditions. The lower curve represents the 1025 curve, scaled by a factor of 0.943 (again determined through regression analysis). Note the good agreement between the scaled 1025 rule and the CA-15 results. This process was repeated for each of the high alloy grades studied, and the scale factors were collected and tabulated along with the C&LA cast alloy multipliers in Table 2. Note that all the high alloy multipliers are relatively close to unity. The largest deviations from unity, for HP and low carbon CF-8M, are only ten pct. This indicates that the feeding distances of the high alloy grades considered are all very similar to those of C&LA steels, if all other casting conditions are the same. With the exception of high carbon CF-8M, all the alloys studied have slightly shorter feeding distances than AISI 1025 steel. In their study, Varga *et al.*[17] found that most of these alloys had longer feeding distances than C&LA steel. This is likely due to the larger superheats typically used for high alloy steels than for C&LA steels; pouring temperatures are often similar, but high alloy steels have significantly lower liquidus temperatures (due to the additional alloying elements) than do C&LA steels. Evidence of the higher superheat can be seen from the data in Table 1; the average superheat from the high alloy casting trials was 158°C (284°F). Considering the superheat multipliers in Table 2, a 158°C (284°F) superheat has a multiplier of almost 1.2, or nearly a 20 pct increase in feeding distance due to the superheat alone.

As with the C&LA rule development, each high alloy grade studied was also simulated, over the whole range of *T* and *W/T* considered, with superheats ranging from 30°C to 250°C (54°F to 450°F), with different sand mold materials, and with drag chills and end chills. Simulation results were compared with values generated using the end effect feeding distance rule (Figure 16 or Equation (1)) with the appropriate multipliers (Equation (2) and Table 2), to ensure that the superheat, mold material and chill multipliers from the C&LA rule development were also valid for high alloy steels. An example of this is provided in Figure 19. The middle curve in this figure is the end effect feeding distance rule for the base casting conditions (Figure 16 or Equation (1)). The lower curve is the same feeding distance rule scaled by the CF-8M (0.06 pct carbon) multiplier, and the upper curve accounts for both CF-8M and a superheat of 100°C (180°F). The open symbols in this plot are simulation results for 5.08 cm (2 in.) thick CF-8M plates cast in furan sand molds; the diamonds represent a superheat of 60°C (108°F), and the circles represent a superheat of 100°C (180°F). Note the good agreement between the simulation results and the corresponding feeding distance rule values. Good agreement was also found for the cooling condition and sand mold material multipliers in Table 2.

A comparison between the new high alloy feeding distance rule and current SFSA rules[29] is provided in Figure 20. The uppermost curve in this figure represents the new feeding distance rule over a range of *W/T* for CF-8M (0.06 pct carbon) cast in a furan sand mold, with a superheat of 160°C (288°F). As mentioned earlier, this value represents the average superheat from the high alloy casting trials (see Table 1); although Varga *et al*.[17] neither considered nor reported the superheats used in their casting trials, it can be expected that they were of the same order. Again, the new rule was developed using the average feeding distance values for thicknesses ranging from T = 2.54 to 30.5 cm (1 to 12 in.), and is valid over this thickness range. The three lower curves, which are taken from the high alloy risering rules in *Risering Steel Castings*,[29] are only applicable to 2.54 cm (1 in.) thick sections. It should be noted that, in *Risering Steel Castings*, there is only one feeding distance rule provided for 2.54 cm (1 in.) thick sections for all the high alloy grades listed in this figure. However, this handbook measures feeding distance from the center of the riser to the edge of the casting (see Figure 1). In order to convert the feeding distance from the SFSA high alloy definition to the present definition (shown in Figure 20), it is necessary to calculate the appropriate riser size for each casting geometry. *Risering Steel Castings* provides different riser sizing rules for three categories of high alloy steels; these different rules lead to the three lower curves seen in Figure 20. In this example, the new rule feeding distance is seen to be significantly longer over the entire range of *W/T* than feeding distances determined with the existing rules. There are two reasons for this. First, Varga *et al*.[16-19] developed their rules based solely on empirical analysis; they determined feeding distances primarily by sectioning castings with centerline shrinkage, and measuring the riser zone (distance from the riser to the beginning of the shrinkage) and end zone (distance from end of shrinkage to the end of the casting). They added these two values (plus the riser radius) to determine the feeding distance. However, the feeding distance (FD_{HA} in Figure 1) can only be computed as the sum of the riser radius, riser zone length and end zone length for the longest sound casting before shrinkage forms (e.g., Figure 15). As noted by Pellini *et al*.,[3,6] if the casting length exceeds the maximum length of a sound casting and shrinkage forms (e.g., Figure 11), the shrinkage region encroaches on the riser zone, which reduces the riser zone length from its maximum value. This yields a conservative estimate of the feeding distance. Also, *Risering Steel Castings* only provides a single feeding distance chart for all high alloy grades. Varga et al.[17,18] developed such charts for several grades; when this work was condensed into *Risering Steel Castings*, only the most conservative feeding distance chart was provided, so that it would be valid for all alloys.

In summary, through high alloy casting trials and extensive use of casting simulation, it was determined that the low alloy feeding distance rules developed in the authors' previous work[9,10,30] are also applicable to the high alloy grades considered in this work, provided that the appropriate high alloy grade multiplier (given in Table 2) is used. The present work only discussed the end effect feeding distance rule, applicable to single top risers. However, the previous work also presented rules for lateral feeding and side risers.[10,30] In order to use these lateral feeding or side riser rules for high alloy steels, one simply needs to replace $(FD/T)_{\text{base case}}$ in Equation (2) with the corresponding feeding distance rule, and apply the appropriate multipliers. One clarification is in order, however: if distances are being computed for lateral feeding between two risers, and a drag chill is being used, one should use the end effect feeding distance rule in Equation (1) and the drag chill multiplier from Table 2 to determine this distance. The reason for this is that a drag chill essentially creates an artificial end zone, which approximates an end effect (which is why the drag chill multiplier is close to unity). The end chill and drag chill dimensions recommended for application of these feeding distance rules are given in the previous work.[10,30]

6 CALCULATION OF RISER SIZE

As stated in the introduction, the only known extensive effort to develop riser sizing rules for high alloy steels was performed by Varga *et al*.;[16-19] this work was later incorporated into the SFSA handbook *Risering Steel Castings*,[29] along with the C&LA riser sizing rules developed by Bishop *et al*.[26] A direct comparison of the C&LA riser sizing rule of Bishop *et al*. and the high alloy rules of Varga *et al*. is shown in Figure 21. This figure gives the riser-volume-to-casting-volume ratio as a function of the shape factor of the casting section the riser is intended to feed. From this figure, it is evident that the high alloy riser sizing rules call for significantly larger riser sizes for a given shape factor. To understand why this is the case, it is necessary to review how these rules were developed.

Bishop *et al*.[26] developed their C&LA riser sizing rules based on a set of plate casting trials. These trials used open top risers, with a wide range of plate sizes and riser height-to-diameter ratios. Using radiographs of the riser pipe, they defined the minimum riser size as one where the tip of the riser pipe just met the riser-casting contact surface. Defining the safety margin (SM) to be the distance from the riser-casting contact surface to the tip of the riser pipe (see Figure 22), the minimum riser requirement of Bishop *et al*. can also be described as a riser having a safety margin of zero (SM = 0). Through experimentation, they found that the minimum riser height could be determined from any casting by determining its safety margin, provided that the safety margin did not exceed one or two inches. The minimum riser height was found by simply subtracting the safety margin from the original riser height (i.e., $H_{R,min} = H_R - SM$). Note that if the riser pipe extended into the casting, the safety margin was negative, so the minimum riser height was larger than the original height. Bishop *et al*. used this new minimum riser height ($H_{R,min}$) with the original riser diameter (D_R) to determine the minimum riser volume, and in this manner developed a plot of riser-volume-to-casting-volume ratio versus shape factor. The experimental data in this plot fall in a band of riser volumes for each shape factor; Bishop et al. included an upper-bound curve (above which the riser is too large) and a lower-bound curve (below which the riser is too small) for the experimental data. The C&LA riser size curve shown in Figure 21, developed by Spiegelberg[12], represents the upper-bound curve of this band. The nomograph given to size C&LA risers in *Risering Steel Castings*[29] was developed from this upper-bound curve.

Varga *et al*.[16-17] developed their high alloy riser sizing rules using a methodology similar to that of Bishop *et al*., but with several important differences. They also performed casting trials, for the high alloy steels they were investigating, and used riser pipe radiographs to determine the safety margin. For their study, however, all of their risers were blind top risers (both with and without cracker cores) that had height-to-diameter ratios of unity (i.e., $D_R = H_R$). When they measured the safety margin, then, they modified both the riser height and diameter to determine the minimum riser size (i.e., $H_{R,min} = H_R - SM$ and $D_{R,min} = D_R - SM$). An important note regarding this procedure, however, is that most of their original risers were too small. As a result, most of their riser pipes extended into the castings (up to about 1.27 cm (0.5 in.)), producing negative safety margins, as illustrated in Figure 23. Thus, when they calculated minimum riser size, they typically increased both the riser height and diameter, when it was really only necessary to increase the height (according to the methodology experimentally established by Bishop *et al.*[26]). This produced larger than necessary riser volumes.

Also analogous to Bishop *et al.*, Varga *et al.* then plotted the experimental minimum riser volumes as a function of shape factor. The results for each alloy grade were plotted separately, and if the alloy was cast both with and without cracker cores, two plots were made for that alloy grade to separate this effect as well. Varga *et al.* then represented the band of experimental data in each of these plots by using the upper-bound curve, analogous to the C&LA curve shown in Figure 21. When an alloy grade had results both with and without cracker cores, they condensed this information by using the more conservative of the two to represent that alloy grade. The results for blind risers with cracker cores were more conservative, as they tend to produce deeper riser pipes. This is illustrated through MAGMASOFT casting simulation results in Figure 24. This figure shows riser pipes for a 2.54 by 38.1 by 35.6 cm (1 by 15 by 14 in.) CA-15 plate casting with a riser having both diameter and height equal to 7.64 cm (2.9375 in.). Note that the open riser has a larger safety margin than either blind riser case. The blind riser with the cracker core has a slightly deeper riser pipe than the vented blind riser without a cracker core; this trend is seen in industry as well. However, the difference between the riser pipes in Figures 24b and 24c is small enough that it could be considered a grid effect; a finer grid would be required to verify this difference. Figure 24c corresponds to one of the plates cast in the trials of Varga *et al.*; they measured a safety margin of -0.76 cm (–0.3 in.). The discrepancy between the measured value and the simulated value of –0.20 cm (–0.08 in.) is likely due to the fact that Varga *et al.* did not report the superheat used to produce these plates; a superheat of 150ºC (270ºF) was used in the simulations shown in Figure 24, but if a superheat of 200ºC (360ºF) is used in the case shown in Figure 24c, the simulated safety margin is –0.69 cm (-0.27 in.). It should be noted that the simulated riser pipes produced by MAGMASOFT[34] are considered reliable in industry; a comparison between simulations and the casting trial results of Bishop *et al.*[26] (who did report superheats) for 1025 steel castings is shown in Figure 25. Finally, two other factors of safety were built in to the riser sizing rules of Varga *et al*. First, they combined the alloys they considered into three groups (the three high alloy groups shown in Figure 21), taking the most conservative curve from each group to represent the entire group. Finally, when they had reduced their data down to riser sizing curves for three groups, they increased the riser sizes further by adding a safety margin of 0.64 cm (0.25 in.) to define their minimum riser size.

Also shown in Figure 21 (as open circles) are simulation values of the minimum riser size for several shape factors. These simulations were performed with AISI 1025 steel in a green sand mold, with a 120ºC (216ºF) superheat. All risers in the simulations were open top risers with height-to-diameter ratios of unity, and the minimum riser size was defined as a riser with $SM = 0$. This was determined by iteratively changing the riser size until the simulation resulted in a zero safety margin. Note that the simulation data agree very well with the C&LA riser sizing curve of Bishop *et al.*, and that the simulation data are slightly less conservative. This is not surprising, considering that the C&LA curve shown was taken as the upper-bound curve from the $SM = 0$

data in the work of Bishop *et al*.

As stated earlier, the C&LA riser sizing rule developed by Spiegelberg[12], based on the work of Bishop *et al*.,[26] is considered adequate for C&LA steels. The changes made by Varga *et al*.[16-17] in the methodology of Bishop *et al*. result in riser sizing rules that are too conservative. In an effort to demonstrate this, the minimum riser sizes for the casting trial data of Varga *et al*. were recalculated, using the same riser sizing methodology that was used by Bishop *et al*. (i.e., determining the minimum riser dimensions by changing the riser height based on the safety margin, but continuing to use the original riser diameter; also, designing the minimum riser size for SM = 0 rather than 0.64 cm (0.25 in.)). The results for each alloy were combined into the same groups used by Varga *et al*., taking the most conservative results from each group. This information is plotted in Figure 26. Comparing Figure 26 to Figure 21, note that the re-calculated high alloy blind riser sizes are considerably less conservative than those of Varga *et al*. The results for low carbon HF, HH, CA-15 and CF-8 are, in fact, nearly coincident with the C&LA curve for open top risers. The curves for the other high alloy grades are not very far above the C&LA curve for open top risers.

The issue of whether or not different riser sizing curves are truly required for different high alloy grades was investigated further. As mentioned in the discussion of Figure 10b, due to the differences in density curves among the alloy grades, the differences in their solidification shrinkage can be significant. This could indicate that riser pipe depths may be different for different alloys, and that different riser sizes for the same casting section may be required. However, as illustrated in Figure 27, simulation results indicate that this is not the case. This figure shows minimum riser sizes for simulations of plate castings of various sizes and alloys. All other casting conditions were held constant for these simulations. As with the simulation results shown in Figure 21, the minimum riser sizes were calculated using open top risers with $H_R/D_R = 1$, and iterating on the riser size until a safety margin of zero was achieved. Notice that the riser sizes for a given plate size are essentially constant, regardless of the alloy; also note that AISI 1025 is included along with the high alloy grades. This indicates that, for open top risers, as long as the casting conditions other than alloy grade are held constant, the same size riser can be used, regardless of the alloy. Therefore, the C&LA curve shown in Figure 26 can be used to size high alloy open top risers as well as C&LA open top risers. How is this possible, considering that the solidification shrinkage in this figure varies from about 2.8 pct to 4.5 pct? This is explained in Figure 28, which shows risers resulting from another set of simulations. All of these simulations are for a 2.54 by 12.7 by 35.6 cm (1 by 5 by 14 in.) plate, with a vented blind top riser (D_R = 6.70 cm (2.6375 in.) and H_R = 7.46 cm (2.9375 in.)). The simulation was performed for various alloys, all cast in green sand with a 100°C (180°F) superheat. Notice that these riser pipes have different shapes; some wider and some narrower. However, the safety margin for all these risers is essentially the same. This explains the consistency in riser size, regardless of the amount of solidification shrinkage: the riser pipes take on different shapes, but have about the same depth! This indicates that the size of blind risers is also essentially independent of alloy grade, for C&LA steels and the high alloy grades considered.

In summary, based on this work, the following riser sizing recommendations are made for the high alloy steel grades considered:

- For open top risers: size the riser using the C&LA riser sizing rule given in Figure 26.

- For blind top risers: although the casting trials performed in this work did not use blind risers, simulation with vented blind top risers indicates that the size of blind risers is also independent of the alloy grade, for the high alloy grades considered. Although no blind riser rule was developed, the same practice used in C&LA foundries can be employed: size the riser based on the C&LA rule for open top risers, and then make the riser somewhat taller to account for the deeper pipe that results from a blind riser.

CONCLUSIONS

A new set of feeding distance and riser sizing rules has been developed for high alloy steel grades CF-8M, CA-15, HH, HK and HP. By comparing casting trial results with corresponding casting simulation results, a correlation was developed between the Niyama criterion (a local thermal parameter) and casting soundness. Using this information, extensive casting simulation was used to develop feeding distance rules for a wide range of casting conditions. It was found that the feeding distance rules developed in an earlier analogous study for carbon and low-alloy steels could also be used for the high alloy steels considered, provided that the feeding distance was modified by the appropriate high alloy steel grade multiplier. Other multipliers for these feeding distance rules account for superheat, sand mold material, and the use of chills. The new high alloy feeding distance rules, which are valid for section thicknesses ranging from 2.54 to 30.5 cm (1 to 12 in.), are shown to be less conservative than existing feeding distance rules, and are more tailored to the actual casting conditions. In another part of this study, high alloy riser sizing rules were investigated. It was determined that if open top risers are used, the C&LA riser sizing rule (which is less conservative than previously published high alloy riser sizing rules) is applicable for high alloy steels as well. This study also determined that riser size is independent of alloy grade for blind top risers.

ACKNOWLEDGMENTS

This work was prepared with the support of the U.S. Department of Energy (DOE) Award No. DE-FC07-98ID13691. However, any opinions, findings, conclusions, or recommendations expressed herein are those of the authors, and do not necessarily reflect the views of the DOE. We are indebted to Malcolm Blair and Raymond Monroe of the SFSA for their work in helping organize the trials and recruiting members to participate. Most importantly, we thank the participants in the plate casting trials for their substantial time and resource investment in all aspects of the Yield Improvement Program. This work could not have been accomplished without their shared efforts.

REFERENCES

1. *Yield in the Steel Casting Industry – Literature Review and Industry Survey*, Steel Founders' Society of America Special Report No. 30, 1998.
2. C. Beckermann, X. Shen, J. Gu and R.A. Hardin: "A Computational Study of Feeding Rules and Yield Improvement Techniques," *1997 SFSA Technical and Operating Conference*, 1997.
3. H.F. Bishop and W.S. Pellini: *Am. Foundrymen's Soc. Trans.*, 1950, vol. 58, pp. 185-197.
4. H.F. Bishop, E.T. Myskowski and W.S. Pellini: *Am. Foundrymen's Soc. Trans.*, 1951, vol. 59, pp. 171-180.

5. E.T. Myskowski, H.F. Bishop and W.S. Pellini: *Am. Foundrymen's Soc. Trans.*, 1952, vol. 60, pp. 389-400.
6. W.S. Pellini: *Am. Foundrymen's Soc. Trans.*, 1953, vol. 61, pp. 61-80.
7. E.T. Myskowski, H.F. Bishop and W.S. Pellini: *Am. Foundrymen's Soc. Trans.*, 1953, vol. 61, pp. 302-308.
8. C.W. Briggs: *Determination of the Factors Influencing Riser Efficiency Part II, The Distance Risers Will Feed Uniformly Thick Sections*, Steel Founders' Society of America Research Report No. 30, Technical Research Committee Report, 1953.
9. K.D. Carlson, S. Ou, R.A. Hardin and C. Beckermann: *Metall. Mater. Trans. B*, 2002, vol. 33B, pp. 731-740.
10. S. Ou, K.D. Carlson, R.A. Hardin and C. Beckermann: *Metall. Mater. Trans. B*, 2002, vol. 33B, pp. 741-755.
11. W.D. Spiegelberg: M.S. Thesis, Case Western Reserve University, Cleveland, OH, 1968.
12. W.D. Spiegelberg: Ph.D. Thesis, Case Western Reserve University, Cleveland, OH, 1970.
13. R. Maier: M.S. Thesis, Case Western Reserve University, Cleveland, OH, 1972.
14. W.P. Ghun: M.S. Thesis, Case Western Reserve University, Cleveland, OH, 1974.
15. E. Niyama, T. Uchida, M. Morikawa and S. Saito: *Am. Foundrymen's Soc. Int. Cast Met. J.*, 1982, vol. 7 (3), pp. 52-63.
16. J. Varga, Jr. and H.W. Lownie, Jr.: Summary Report on Solidification and Feeding of High-Alloy Castings, Alloy Casting Institute, April 1955.
17. J. Varga, Jr., A.J. Stone and H.W. Lownie, Jr.: Summary Report on Solidification and Feeding of High-Alloy Castings, Alloy Casting Institute, September 1956.
18. J. Varga, Jr., A.J. Stone and H.W. Lownie, Jr.: Summary Report on Solidification and Feeding of High-Alloy Castings, Alloy Casting Institute, September 1957.
19. J. Varga, Jr., A.J. Stone and H.W. Lownie, Jr.: Summary Report on Solidification and Feeding of High-Alloy Castings, Alloy Casting Institute, June 1958.
20. N. Chvorinov: *Giesserei*, 1940, vol. 27, pp. 177-225.
21. N. Janco: "Calculating Sizes of Gates and Risers," *Am. Foundrymen's Soc. Trans.*, 1947, vol. 55, pp. 296-300.
22. N. Chvorinov: "Control of the Solidification of Castings by Calculation," *Foundry Trade Journal*, 1939, pp. 95-98.
23. Wlodawer: *Directional Solidification of Steel Castings*, 1st English ed., Pergamon Press Inc., Long Island, New York, 1966, pp. 1-15.
24. R.W. Ruddle: *Am. Foundrymen's Soc. Trans.*, 1971, vol. 79, pp. 269-280
25. J.B. Caine: "A Theoretical Approach to the Problem of Dimensioning Risers," *Am. Foundrymen's Soc. Trans.*, 1949, vol. 57, pp. 492-501.
26. H.F. Bishop, E.T. Myskowski and W.S. Pellini: "A Simplified Method for Determining

Riser Dimensions," *Am. Foundrymen's Soc. Trans.*, 1955, vol. 63, pp. 271-281.

27. T.E. Morthland, P.E. Byrne, D.A. Tortorelli and J.A. Dantzig: *Metall. Mater. Trans. B*, 1995, vol. 26B, pp. 871-895.
28. S. Ou: Ph.D. Thesis, The University of Leoben, Leoben, Austria, 1998.
29. *Risering Steel Castings*, Steel Founders' Society of America, Barrington, Illinois, 1973.
30. *Feeding & Risering Guidelines for Steel Castings*, Steel Founders' Society of America, Barrington, Illinois, 2001.
31. *ASTM E94-00*, Annual Book of ASTM Standards, Volume 03.03: Nondestructive Testing, American Society for Testing of Materials, 2002.
32. *ASTM E446-98*, Annual Book of ASTM Standards, Volume 03.03: Nondestructive Testing, American Society for Testing of Materials, 2002.
33. K. Carlson, S. Ou, R.A. Hardin and C. Beckermann: *Int. J. Cast Metals Res.*, 2001, vol. 14 (3), pp. 169-183.
34. *MAGMASOFT*, MAGMA GmbH, Kackerstrasse 11, 52072 Aachen, Germany.
35. *AFSolid*, AFS, Inc., 505 State Street, Des Plaines, Illinois, 60016, USA.
36. *Development of a Methodology to Predict and Prevent Leaks Caused by Microporosity in Steel Castings*, Steel Founders' Society of America Research Report No. 110, 2001.
37. J. Miettinen: *Metall. Trans. B*, 1997, vol. 28B, pp. 281-297.
38. J. Miettinen and S. Louhenkilpi: *Metall. Trans. B*, 1994, vol. 25B, pp. 909-916.

Table 1 Experimental data from the high alloy plate casting trials.

*W/T**	Steel Alloy	Foundry	*L* (in.)	D_R (in.)	H_R (in.)	*FL* (in.)	Pouring *T* (ºC)	Superheat (ºC)	Sand Mold	X-ray level
2	CF-8M	A	3.25	1.5	7	1.80	1593.3	161.1	furan	0
2	CF-8M	A	3.25	1.5	7	1.80	1604.4	172.2	furan	0
2	CF-8M	A	3.25	1.5	7	1.80	1598.9	166.7	furan	0
2	CF-8M	A	3.25	1.5	7	1.80	1587.8	155.6	furan	0
2	CF-8M	A	3.25	1.5	7	1.80	1596.1	163.9	furan	0
2	CF-8M	A	3.75	1.5	7	2.29	1557.2	122.6	furan	0
2	CF-8M	A	3.75	1.5	7	2.29	1554.4	119.8	furan	0
2	CF-8M	A	3.75	1.5	7	2.29	1571.1	136.5	furan	0
2	CF-8M	A	3.75	1.5	7	2.29	1560.0	125.4	furan	0
2	CF-8M	A	3.75	1.5	7	2.29	1562.8	128.2	furan	0
2	CF-8M	A	4.75	1.5	7	3.28	1576.7	142.1	furan	0
2	CF-8M	A	4.75	1.5	7	3.28	1571.1	136.5	furan	0
2	CF-8M	A	4.75	1.5	7	3.28	1565.6	131.0	furan	0
2	CF-8M	A	4.75	1.5	7	3.28	1586.7	152.1	furan	0
2	CF-8M	A	4.75	1.5	7	3.28	1582.2	147.6	furan	0
2	CF-8M	A	6.75	1.5	7	5.27	1554.4	119.8	furan	1
2	CF-8M	A	6.75	1.5	7	5.27	1548.9	114.3	furan	1
2	CF-8M	A	6.75	1.5	7	5.27	1551.7	117.1	furan	0
2	CF-8M	A	6.75	1.5	7	5.27	1565.6	131.0	furan	1
2	CF-8M	A	6.75	1.5	7	5.27	1555.6	121.0	furan	1
5.5	CF-8M	F	7	4	3.5	7.0	1587.2	133.2	furan	0
5.5	CF-8M	F	7	4	3.5	7.0	1587.2	133.2	furan	0
5.5	CF-8M	F	7	4	3.5	7.0	1587.2	133.2	furan	0
5.5	CF-8M	F	7	4	3.5	7.0	1587.2	133.2	furan	0
5.5	CF-8M	F	7	4	3.5	7.0	1587.2	133.2	furan	0
5.5	CF-8M	F	9.4	4	3.5	9.4	1587.2	133.2	furan	2
5.5	CF-8M	F	9.4	4	3.5	9.4	1587.2	133.2	furan	2
5.5	CF-8M	F	9.4	4	3.5	9.4	1587.2	133.2	furan	0
5.5	CF-8M	F	9.4	4	3.5	9.4	1587.2	133.2	furan	3
5.5	CF-8M	F	9.4	4	3.5	9.4	1587.2	133.2	furan	3
5.5	CF-8M	F	12.3	4	3.5	12.3	1582.8	128.8	furan	3
5.5	CF-8M	F	12.3	4	3.5	12.3	1582.8	128.8	furan	3
5.5	CF-8M	F	12.3	4	3.5	12.3	1582.8	128.8	furan	4
5.5	CF-8M	F	12.3	4	3.5	12.3	1582.8	128.8	furan	2
5.5	CF-8M	F	12.3	4	3.5	12.3	1582.8	128.8	furan	4
5.5	CF-8M	F	15	4	3.5	15.0	1582.8	128.8	furan	5
5.5	CF-8M	F	15	4	3.5	15.0	1582.8	128.8	furan	5
5.5	CF-8M	F	15	4	3.5	15.0	1582.8	128.8	furan	5
5.5	CF-8M	F	15	4	3.5	15.0	1582.8	128.8	furan	5
5.5	CF-8M	F	15	4	3.5	15.0	1582.8	128.8	furan	5
5.5	CF-8M	F	18	4	3.5	18.0	1582.2	128.2	furan	5
5.5	CF-8M	F	18	4	3.5	18.0	1582.2	128.2	furan	5
5.5	CF-8M	F	18	4	3.5	18.0	1582.2	128.2	furan	5
5.5	CF-8M	F	18	4	3.5	18.0	1582.2	128.2	furan	5
5.5	CF-8M	F	18	4	3.5	18.0	1582.2	128.2	furan	5
5.5	CF-8M	K	11	4	4.5	7.41	1586.1	154.1	furan	0
5.5	CF-8M	K	11	4	4.5	7.41	1579.4	147.4	furan	0
5.5	CF-8M	K	11	4	4.5	7.41	1579.4	147.4	furan	0
5.5	CF-8M	K	11	4	4.5	7.41	1580.6	148.6	furan	0
5.5	CF-8M	K	11	4	4.5	7.41	1579.4	147.4	furan	0
5.5	CF-8M	K	12.5	4	4.5	8.85	1587.8	155.8	furan	0
5.5	CF-8M	K	12.5	4	4.5	8.85	1587.2	155.2	furan	0
5.5	CF-8M	K	12.5	4	4.5	8.85	1585.0	153.0	furan	0
5.5	CF-8M	K	12.5	4	4.5	8.85	1579.4	147.4	furan	0
5.5	CF-8M	K	12.5	4	4.5	8.85	1579.4	147.4	furan	0
5.5	CF-8M	K	14	4	4.5	10.3	1598.9	166.9	furan	2
5.5	CF-8M	K	14	4	4.5	10.3	1587.8	155.8	furan	3
5.5	CF-8M	K	14	4	4.5	10.3	1579.4	147.4	furan	0
5.5	CF-8M	K	14	4	4.5	10.3	1580.0	148.0	furan	0
5.5	CF-8M	K	14	4	4.5	10.3	1579.4	147.4	furan	0
5.5	CF-8M	K	16	4	4	12.3	1597.8	165.8	furan	1
5.5	CF-8M	K	16	4	4	12.3	1590.0	158.0	furan	3
5.5	CF-8M	K	16	4	4	12.3	1590.0	158.0	furan	2
5.5	CF-8M	K	16	4	4	12.3	1587.8	155.8	furan	2
5.5	CF-8M	K	16	4	4	12.3	1582.2	150.2	furan	4
5.5	CF-8M	K	18.5	4	4	14.7	1596.1	164.1	furan	3
5.5	CF-8M	K	18.5	4	4	14.7	1593.9	161.9	furan	3
5.5	CF-8M	K	18.5	4	4	14.7	1590.6	158.6	furan	3
5.5	CF-8M	K	18.5	4	4	14.7	1590.0	158.0	furan	3
5.5	CF-8M	K	18.5	4	4	14.7	1581.7	149.7	furan	2
8	CF-8M	A	9	4	6	6.06	1595.6	167.1	furan	0
8	CF-8M	A	9	4	6	6.06	1580.6	152.1	furan	0
8	CF-8M	A	9	4	6	6.06	1590.6	162.1	furan	0
8	CF-8M	A	9	4	6	6.06	1587.8	159.3	furan	0
8	CF-8M	A	9	4	6	6.06	1593.3	164.8	furan	0
8	CF-8M	A	10	4	6	6.94	1558.9	123.4	furan	0
8	CF-8M	A	10	4	6	6.94	1570.6	135.1	furan	0
8	CF-8M	A	10	4	6	6.94	1548.9	113.4	furan	0
8	CF-8M	A	10	4	6	6.94	1560.0	124.5	furan	0
8	CF-8M	A	10	4	6	6.94	1554.4	118.9	furan	0
8	CF-8M	A	11	4	6	7.85	1557.2	125.0	furan	0
8	CF-8M	A	11	4	6	7.85	1551.7	119.5	furan	0
8	CF-8M	A	11	4	6	7.85	1576.7	144.5	furan	0
8	CF-8M	A	11	4	6	7.85	1565.6	133.4	furan	0
8	CF-8M	A	11	4	6	7.85	1582.2	150.0	furan	0
8	CF-8M	A	15	4	6	11.6	1605.6	170.1	furan	0
8	CF-8M	A	15	4	6	11.6	1604.4	168.9	furan	0
8	CF-8M	A	15	4	6	11.6	1593.3	157.8	furan	0
8	CF-8M	A	15	4	6	11.6	1582.2	146.7	furan	0
8	CF-8M	A	15	4	6	11.6	1576.7	141.2	furan	0
8	CF-8M	S	13	4	5.7	9.70	1552.2	120.2	green	4
8	CF-8M	S	13	4	3.8	9.70	1543.3	111.3	green	5
8	CF-8M	S	13	4	5.56	9.70	1553.9	121.9	green	5
8	CF-8M	S	13	4	5.22	9.70	1553.9	121.9	green	5
8	CF-8M	S	15	4	4.6	11.6	1552.2	120.2	green	3
8	CF-8M	S	15	4	4.8	11.6	1541.7	109.7	green	5
8	CF-8M	S	17	4	4.4	13.5	1551.7	119.7	green	5
8	CF-8M	S	17	4	4.8	13.5	1543.3	111.3	green	5
8	CF-8M	S	20	4	4.8	16.4	1551.7	119.7	green	5
8	CF-8M	S	20	4	5.9	16.4	1543.3	111.3	green	5
8	HH	A	11	4	4.25	7.85	1590.6	196.6	furan	0
8	HH	A	11	4	4.25	7.85	1590.6	196.6	furan	0
8	HH	A	11	4	4.75	7.85	1579.4	185.4	furan	0
8	HH	A	11	4	4.75	7.85	1579.4	185.4	furan	0
8	HH	A	13	4	4.125	9.70	1567.2	173.2	furan	1
8	HH	A	13	4	4.125	9.70	1567.2	173.2	furan	0
8	HH	A	13	4	4.25	9.70	1575.6	181.6	furan	0
8	HH	A	13	4	4.25	9.70	1575.6	181.6	furan	1
8	HH	A	15	4	4.5	11.6	1570.6	176.6	furan	2
8	HH	A	15	4	4.5	11.6	1570.6	176.6	furan	1
8	HH	A	15	4	4.5	11.6	1556.1	162.1	furan	1
8	HH	A	15	4	4.5	11.6	1556.1	162.1	furan	2
8	HH	A	17	4	4	13.5	1552.8	158.8	furan	1
8	HH	A	17	4	4	13.5	1552.8	158.8	furan	1
8	HH	A	17	4	4	13.5	1534.4	140.4	furan	1
8	HH	A	17	4	4	13.5	1534.4	140.4	furan	1

Table 1 (continued) Experimental data from the high alloy plate casting trials.

*W/T**	Steel Alloy	Foundry	*L* (in.)	D_R (in.)	H_R (in.)	*FL* (in.)	Pouring *T* (ºC)	Superheat (ºC)	Sand Mold	X-ray level
8	HH	A	20	4	4.25	16.4	1583.9	189.9	furan	1
8	HH	A	20	4	4.25	16.4	1583.9	189.9	furan	2
8	HH	A	20	4	3.75	16.4	1614.4	220.4	furan	4
8	HH	A	20	4	3.75	16.4	1614.4	220.4	furan	2
8	HP	A	11	4	4	7.85	1576.7	231.7	furan	0
8	HP	A	11	4	4	7.85	1576.7	231.7	furan	0
8	HP	A	11	4	4.5	7.85	1586.1	241.1	furan	0
8	HP	A	11	4	4.5	7.85	1586.1	241.1	furan	0
8	HP	A	13	4	4	9.70	1565.6	220.6	furan	2
8	HP	A	13	4	4	9.70	1565.6	220.6	furan	3
8	HP	A	13	4	4.125	9.70	1565.6	220.6	furan	1
8	HP	A	13	4	4.125	9.70	1565.6	220.6	furan	1
8	HP	A	15	4	5	11.6	1597.2	252.2	furan	1
8	HP	A	15	4	5	11.6	1597.2	252.2	furan	2
8	HP	A	15	4	4.5	11.6	1602.8	257.8	furan	2
8	HP	A	15	4	4.5	11.6	1602.8	257.8	furan	2
8	HP	A	17	4	4	13.5	1536.7	191.7	furan	4
8	HP	A	17	4	4	13.5	1536.7	191.7	furan	5
8	HP	A	17	4	4.25	13.5	1585.6	240.6	furan	5
8	HP	A	17	4	4.25	13.5	1585.6	240.6	furan	5
8	HP	A	20	4	4.25	16.4	1598.9	253.9	furan	5
8	HP	A	20	4	4.25	16.4	1598.9	253.9	furan	5
8	HP	A	20	4	4.25	16.4	1607.8	262.8	furan	5
8	HP	A	20	4	4.25	16.4	1607.8	262.8	furan	5

*W/T**	Steel Alloy	Foundry	*L* (in.)	D_R (in.)	H_R (in.)	*FL* (in.)	Pouring *T* (ºC)	Superheat (ºC)	Sand Mold	X-ray level
12	CF-8M	A	4.4	2	6	3.53	1605.6	181.2	furan	0
12	CF-8M	A	4.4	2	6	3.53	1582.8	158.4	furan	0
12	CF-8M	A	4.4	2	6	3.53	1586.7	162.3	furan	0
12	CF-8M	A	4.4	2	6	3.53	1587.8	163.4	furan	0
12	CF-8M	A	4.4	2	6	3.53	1595.6	171.2	furan	0
12	CF-8M	A	5	2	6	4.00	1588.3	163.9	furan	0
12	CF-8M	A	5	2	6	4.00	1610.6	186.2	furan	0
12	CF-8M	A	5	2	6	4.00	1604.4	180.0	furan	0
12	CF-8M	A	5	2	6	4.00	1598.9	174.5	furan	0
12	CF-8M	A	5	2	6	4.00	1593.3	168.9	furan	0
12	CF-8M	A	5.7	2	6	4.58	1585.0	150.3	furan	0
12	CF-8M	A	5.7	2	6	4.58	1582.2	147.5	furan	0
12	CF-8M	A	5.7	2	6	4.58	1578.9	144.2	furan	0
12	CF-8M	A	5.7	2	6	4.58	1585.0	150.3	furan	0
12	CF-8M	A	5.7	2	6	4.58	1587.8	153.1	furan	0
12	CF-8M	A	7.2	2	6	5.89	1593.3	168.9	furan	1
12	CF-8M	A	7.2	2	6	5.89	1598.9	174.5	furan	1
12	CF-8M	A	7.2	2	6	5.89	1587.8	163.4	furan	1
12	CF-8M	A	7.2	2	6	5.89	1582.8	158.4	furan	1
12	CF-8M	A	7.2	2	6	5.89	1600.0	175.6	furan	1
12	CF-8M	A	9.2	2	6	7.73	1567.8	99.8	furan	1
12	CF-8M	A	9.2	2	6	7.73	1571.1	103.1	furan	0
12	CF-8M	A	9.2	2	6	7.73	1565.6	97.6	furan	1
12	CF-8M	A	9.2	2	6	7.73	1577.8	109.8	furan	0
12	CF-8M	A	9.2	2	6	7.73	1568.3	100.3	furan	0

* The *W/T* = 2 and 12 plates are 1.27 cm (0.5 in.) thick, and the *W/T* = 5.5 and 8 plates are 2.54 cm (1 in.) thick.

Table 2 Multipliers used to apply base case feeding rules to other conditions. Base case conditions are listed with the multiplier $C = 1$.

Casting Parameter		Condition Description	Multiplication Factor, C
Sand Mold Material ($C_{\text{sand mold}}$)		furan	1
		green sand	1.09
		zircon	0.96
		chromite	0.88
Cooling Conditions ($C_{\text{cooling conditions}}$)		end effect	1
		end chill	1.19
		drag chill	0.95
Steel Alloy Composition ($C_{\text{cast alloy}}$)	Carbon & Low Alloy	AISI 1025	1
		AISI 4125	0.98
		AISI 1522	0.97
		AISI 4135	0.97
		AISI 4330	0.97
		AISI 8620	0.96
		AISI 8630	0.95
		AISI 4340	0.86
	High Alloy	CF8M – C 0.08	1.036
		HH30	0.985
		CF8M – C 0.06	0.978
		HK44	0.965
		CA15 – C 0.13	0.943
		HP37	0.904
		CF8M – C 0.03	0.900
Superheat ($C_{\text{superheat}}$)		30°C (54°F)	0.94
		60°C (108°F)	1
		90°C (162°F)	1.06
		120°C (216°F)	1.12
		150°C (270°F)	1.18
		250°C (450°F)	1.38

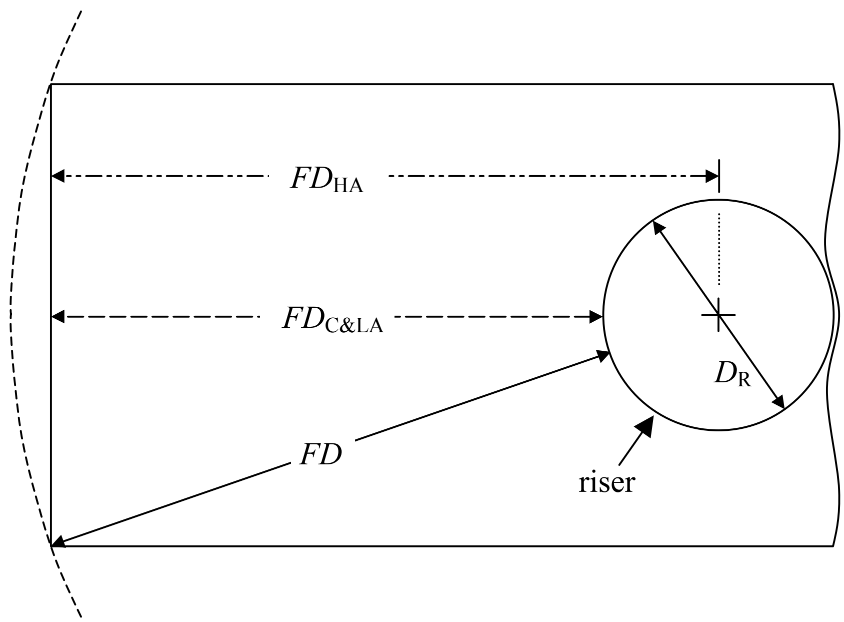

Figure 1 Alternate definitions of feeding distance for previous C&LA ($FD_{C\&LA}$) and high alloy (FD_{HA}) rules, as well as the feeding distance in the current work (FD), which extends from the edge of the riser to the furthest point in the casting.

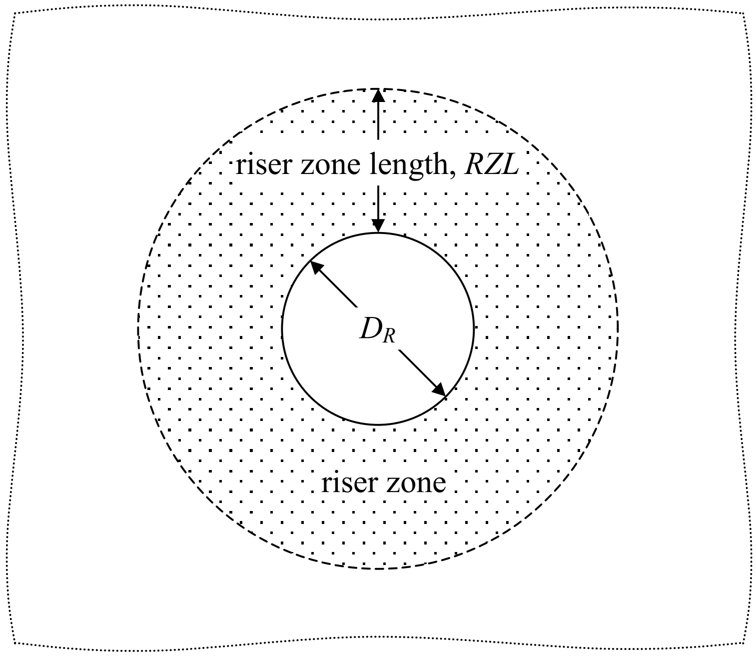

Figure 2 Illustration of the riser zone length *RZL* of a casting section without end effects; note that *RZL* is independent of the riser diameter D_R.

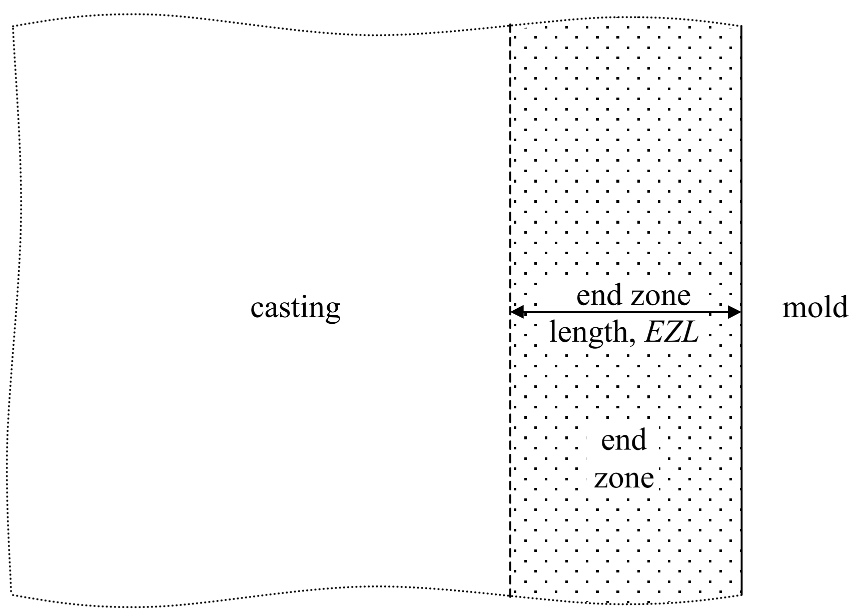

Figure 3 Illustration of the end zone length *EZL* of a casting section.

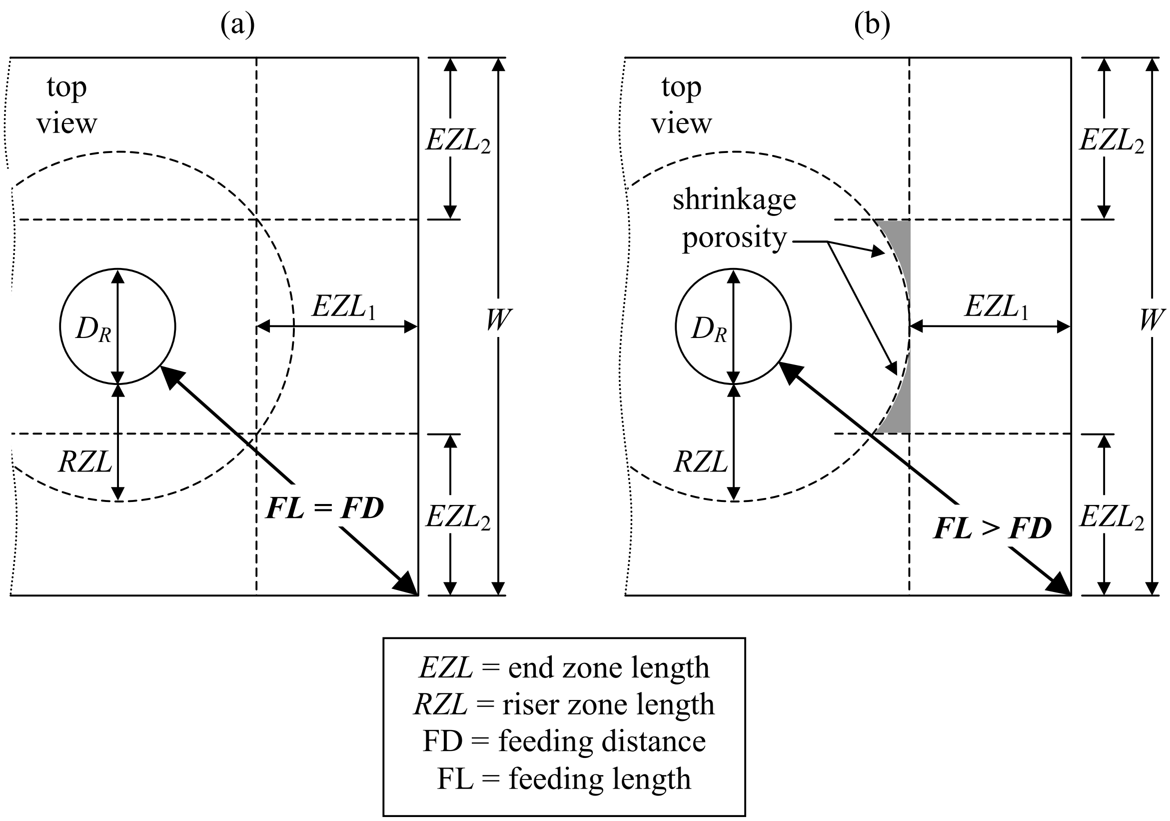

Figure 4 Relationships among *EZL*, *RZL*, *FD* and *FL*: (a) when $FL = FD$, casting section is just covered by riser zones and end zones; (b) when $FL > FD$, shrinkage porosity forms in the shaded sections of casting not covered by riser zones or end zones.

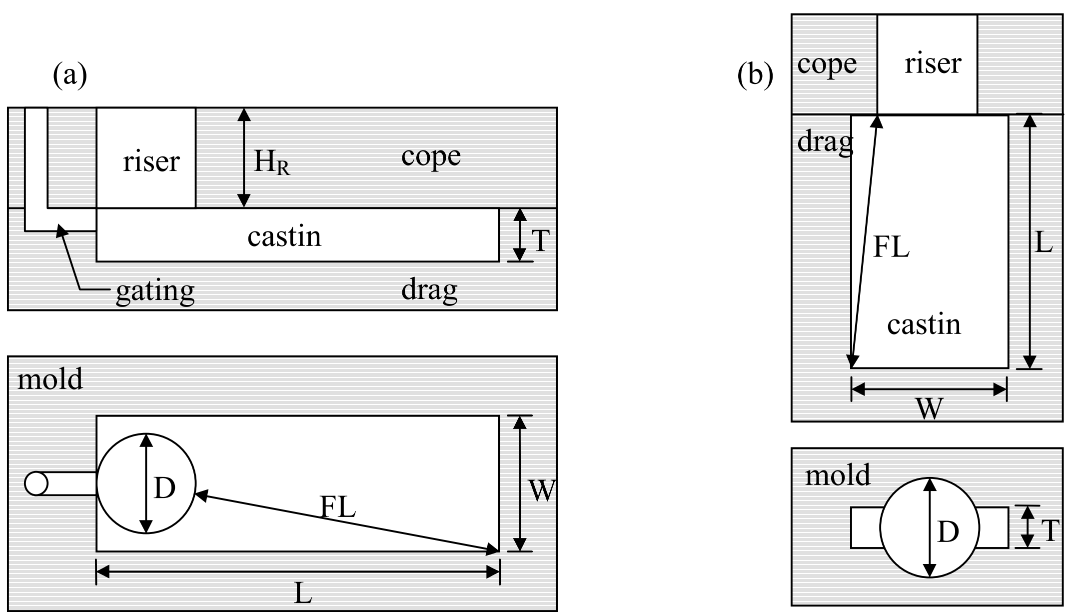

Figure 5 General configuration and nomenclature for (a) horizontal; and (b) vertical plate casting trials.

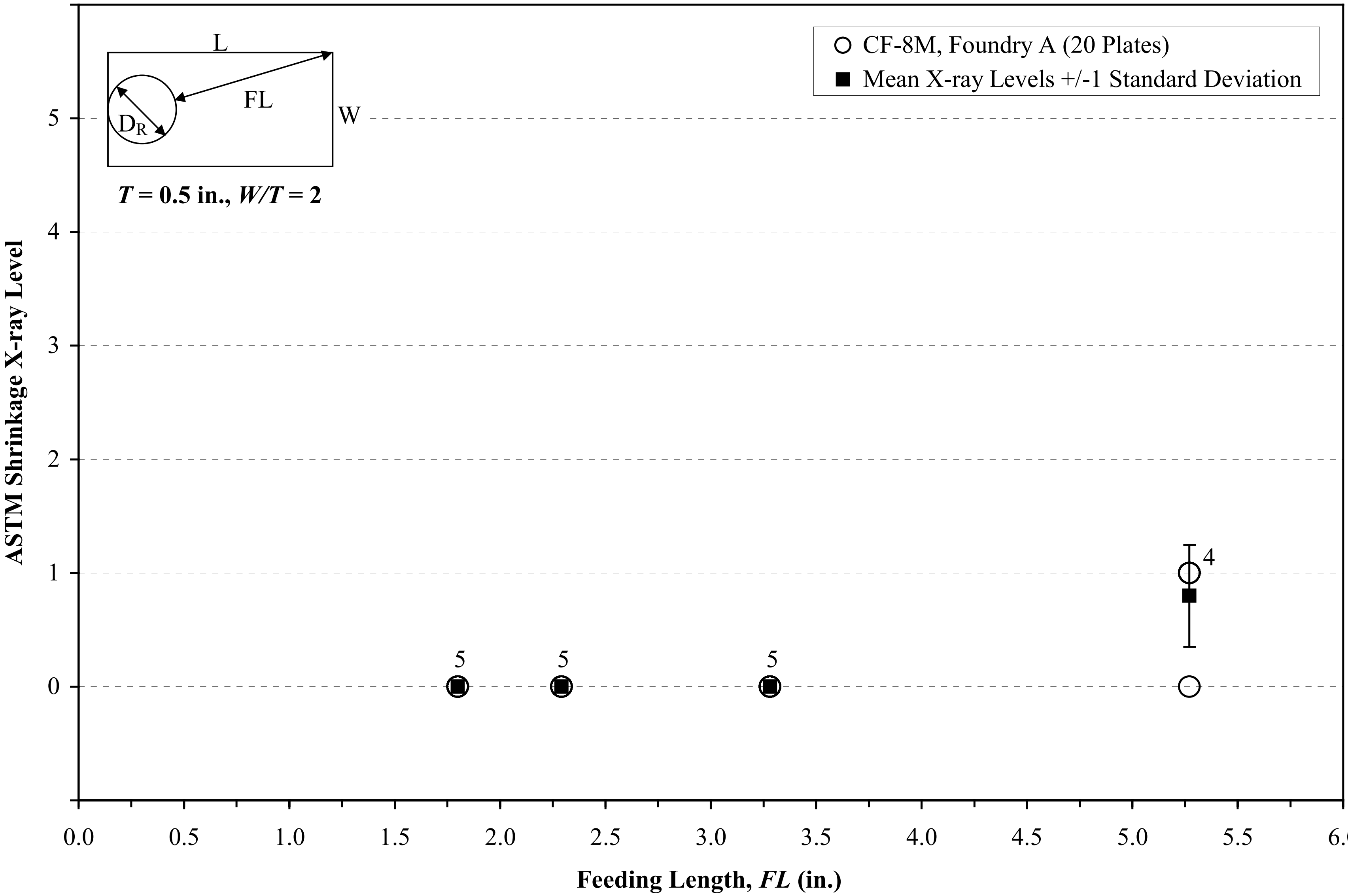

Figure 6 Casting trial results for the *W/T* = 2 [1.27 cm by 2.54 cm (0.5 in. *T* by 1 in. *W*)] plates: soundness versus feeding length.

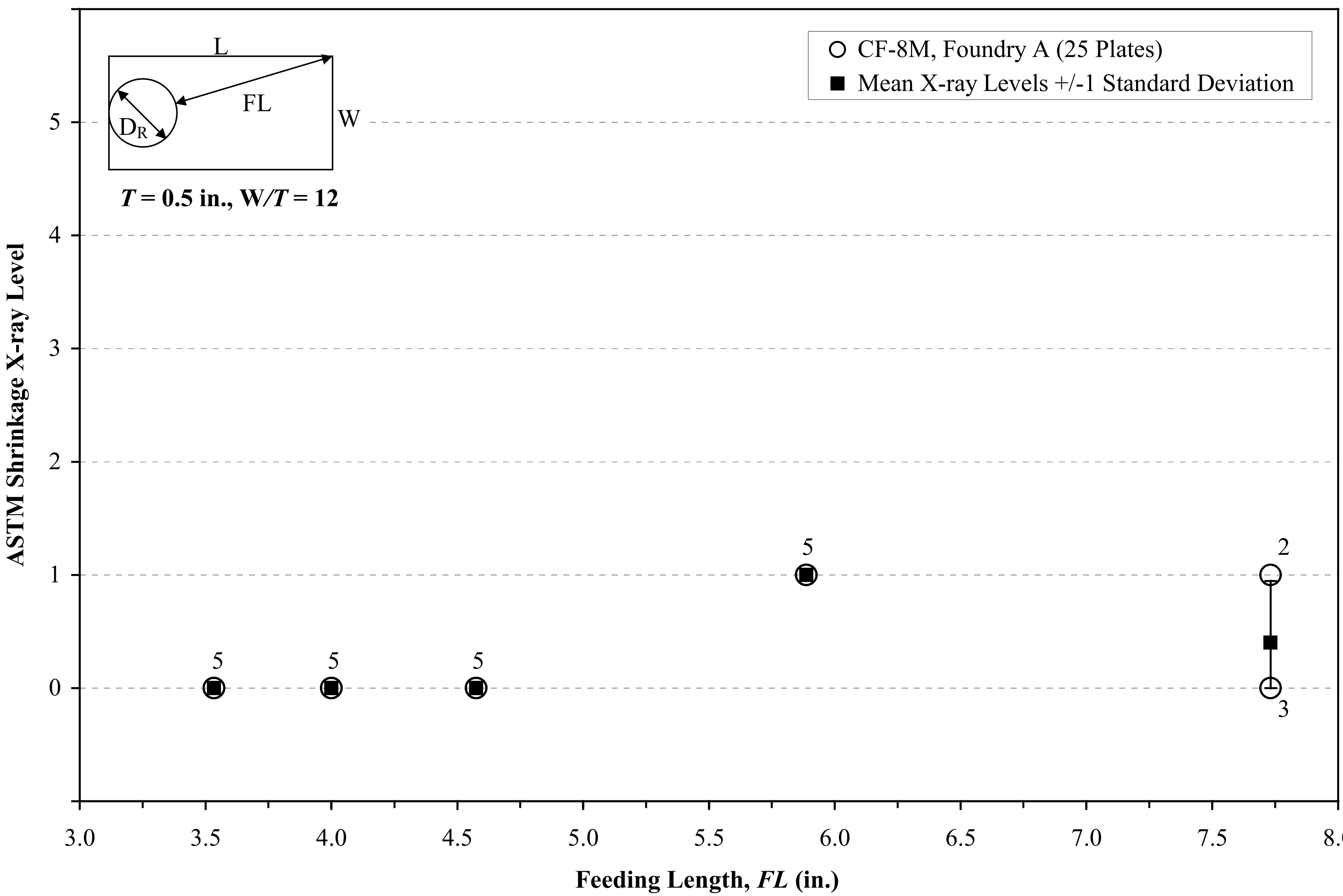

Figure 7 Casting trial results for the *W/T* = 12 [1.27 cm by 15.2 cm (0.5 in. *T* by 6 in. *W*)] plates: soundness versus feeding length.

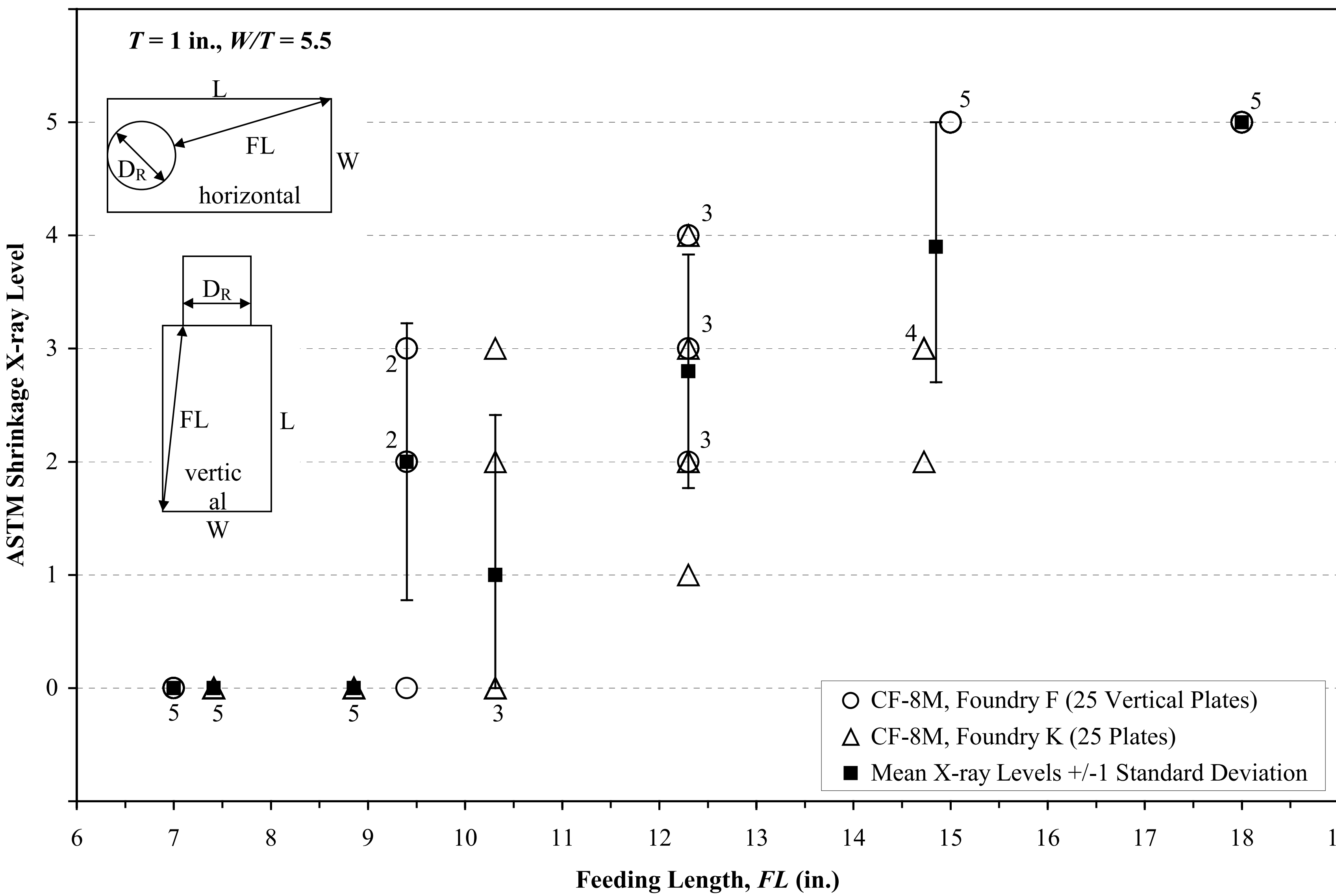

Figure 8 Casting trial results for the $W/T = 5.5$ [2.54 cm by 14.0 cm (1 in. T by 5.5 in. W)] plates: soundness versus feeding length.

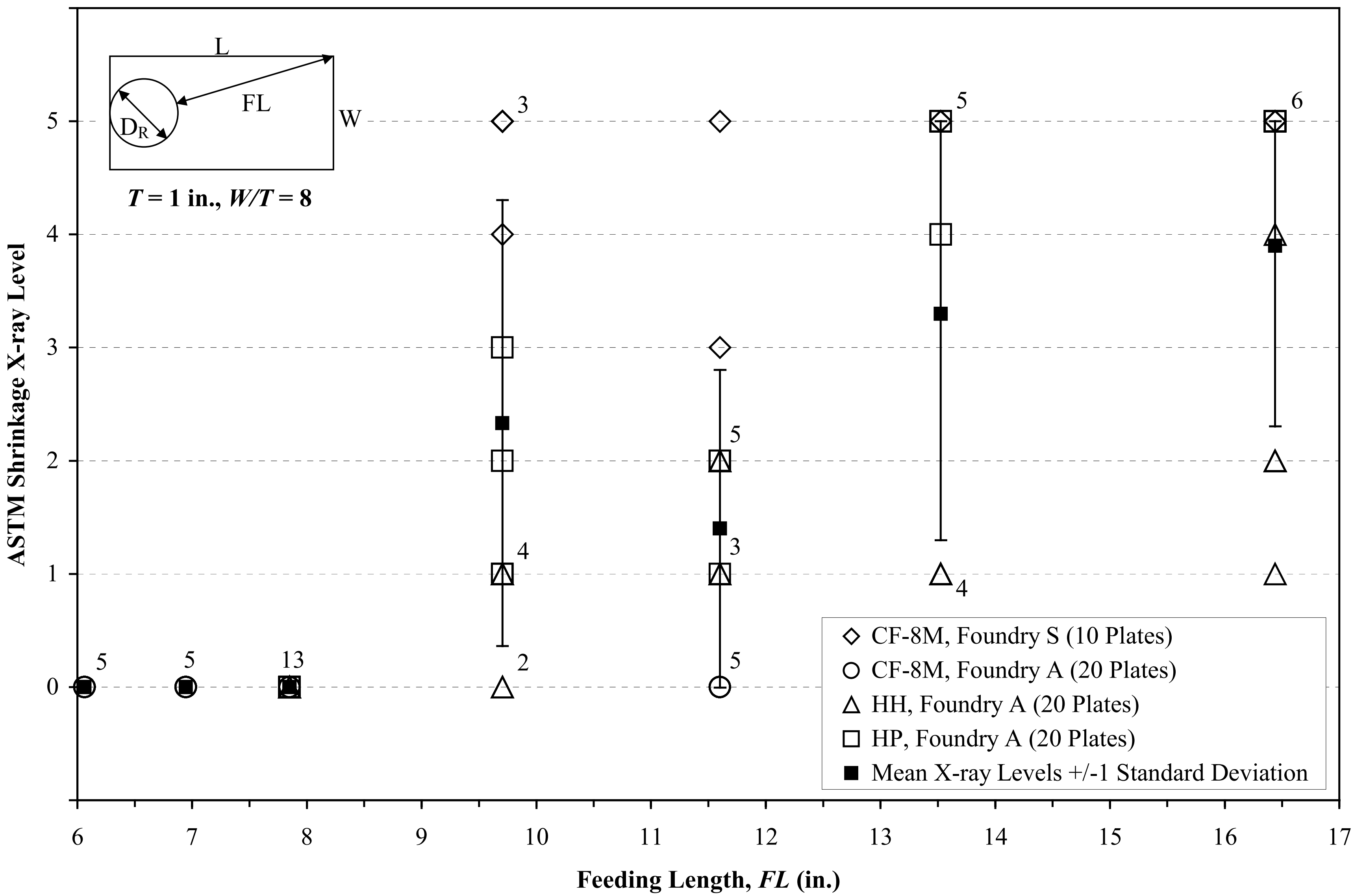

Figure 9 Casting trial results for the *W/T* = 8 [2.54 cm by 20.3 cm (1 in. *T* by 8 in. *W*)] plates: soundness versus feeding length.

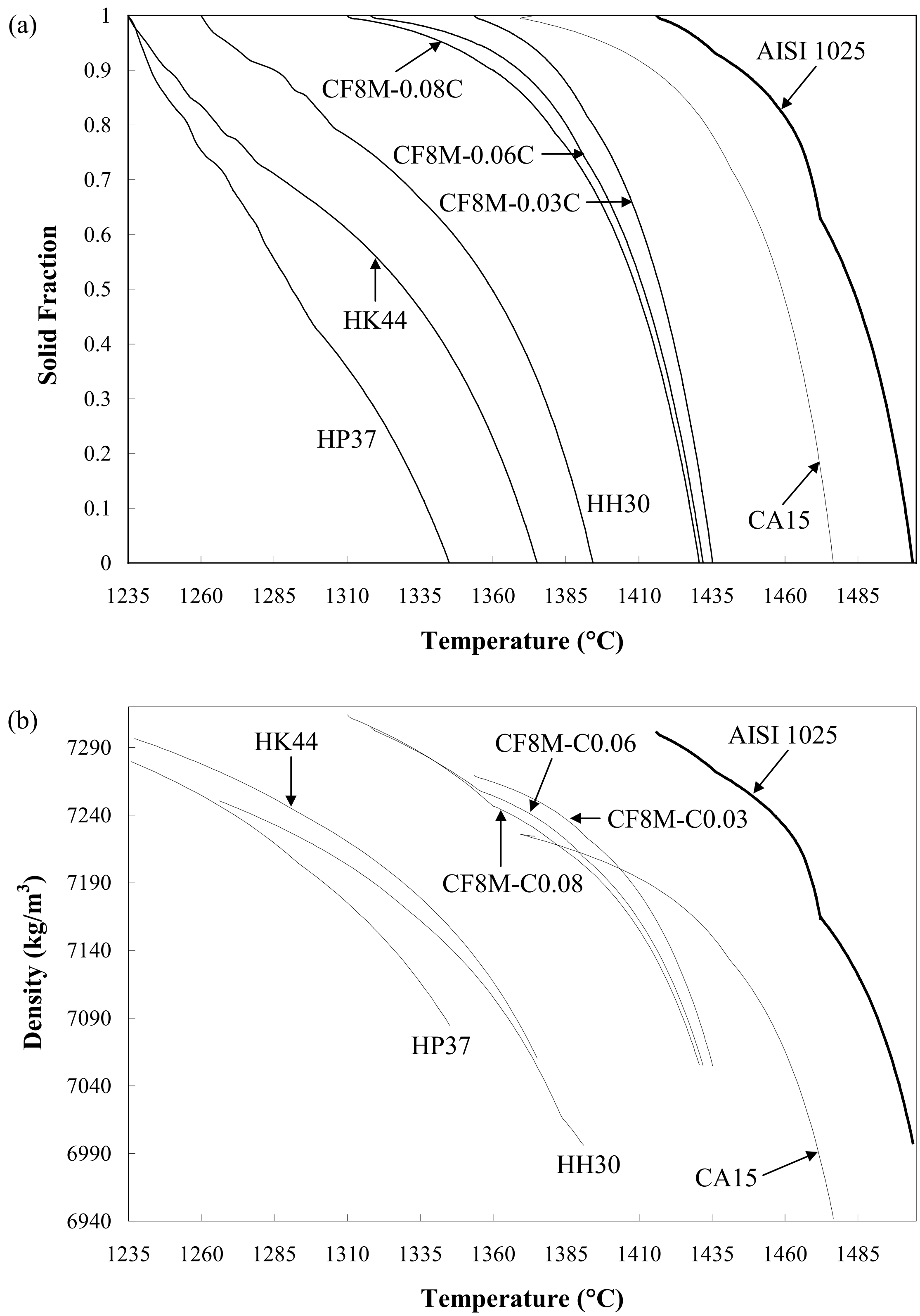

Figure 10 Computed values for alloys of interest: (a) solid fraction and (b) density during solidification.

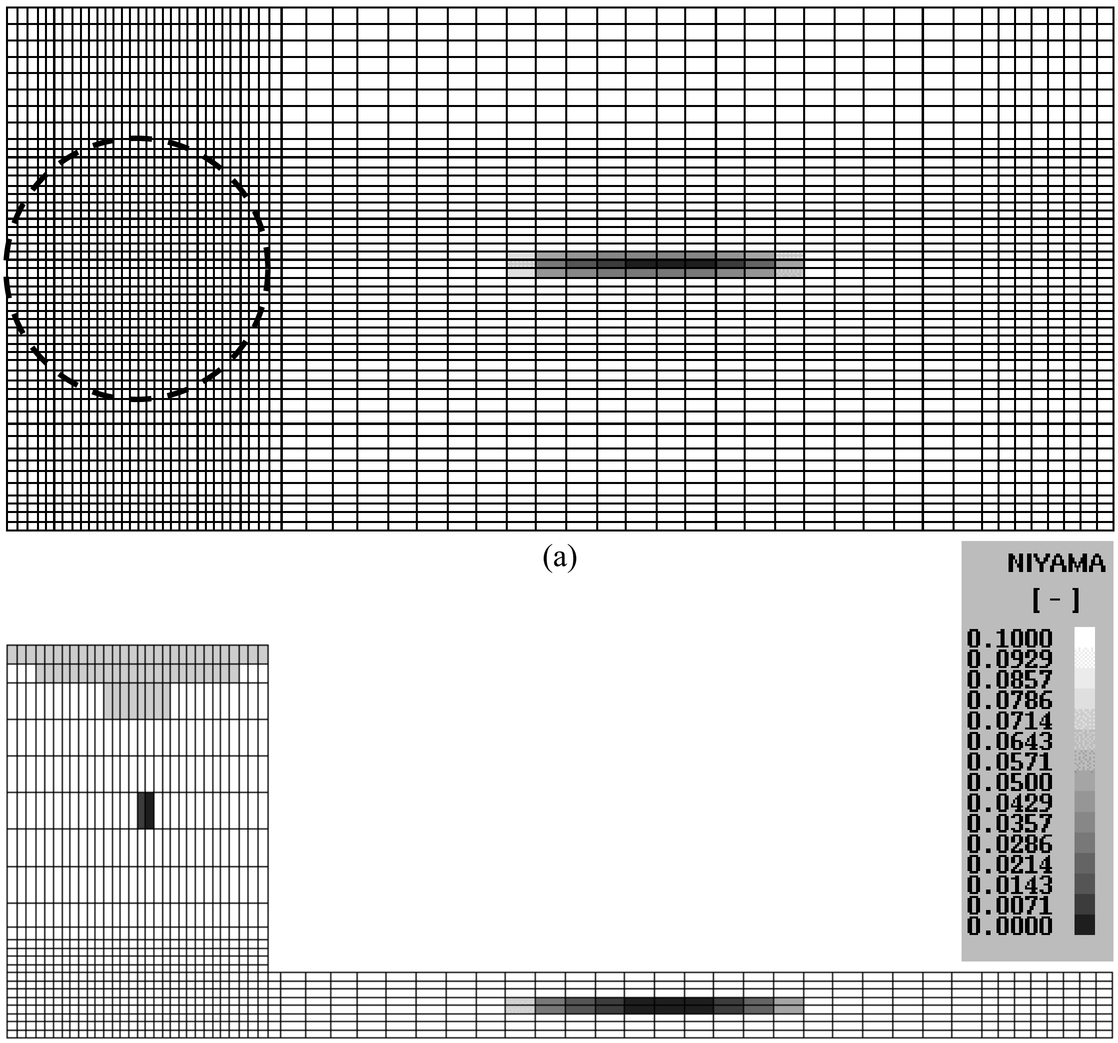

(b)

Figure 11 Niyama value distribution in a 2.54 cm by 20.3 cm by 43.2 cm (1 in. by 8 in. by 17 in.) HH plate: (a) top view of central-thickness cross-section; and (b) side view of central-width cross-section.

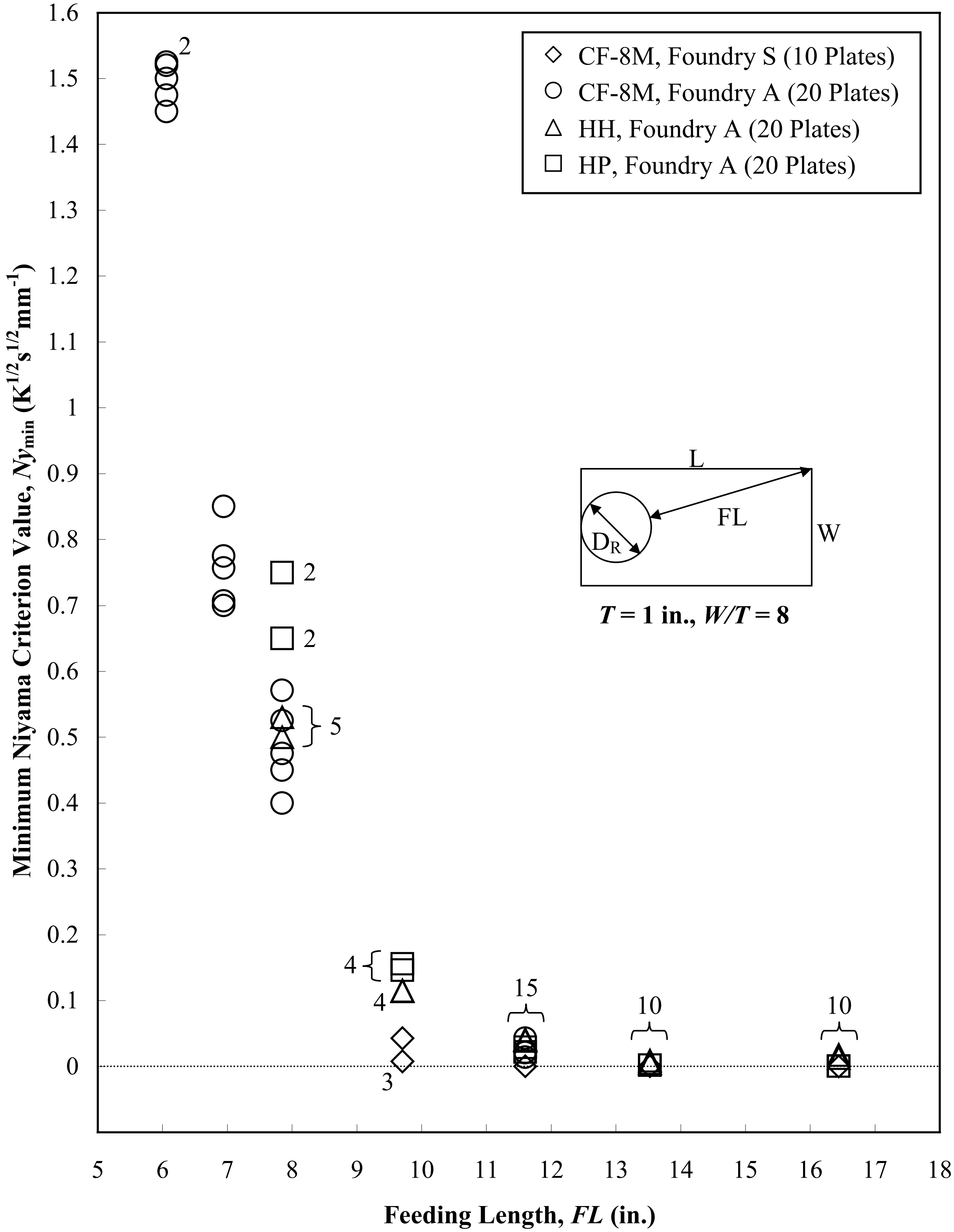

Figure 12 Simulation results for the W/T = 8 plates: minimum Niyama value vs. feeding length.

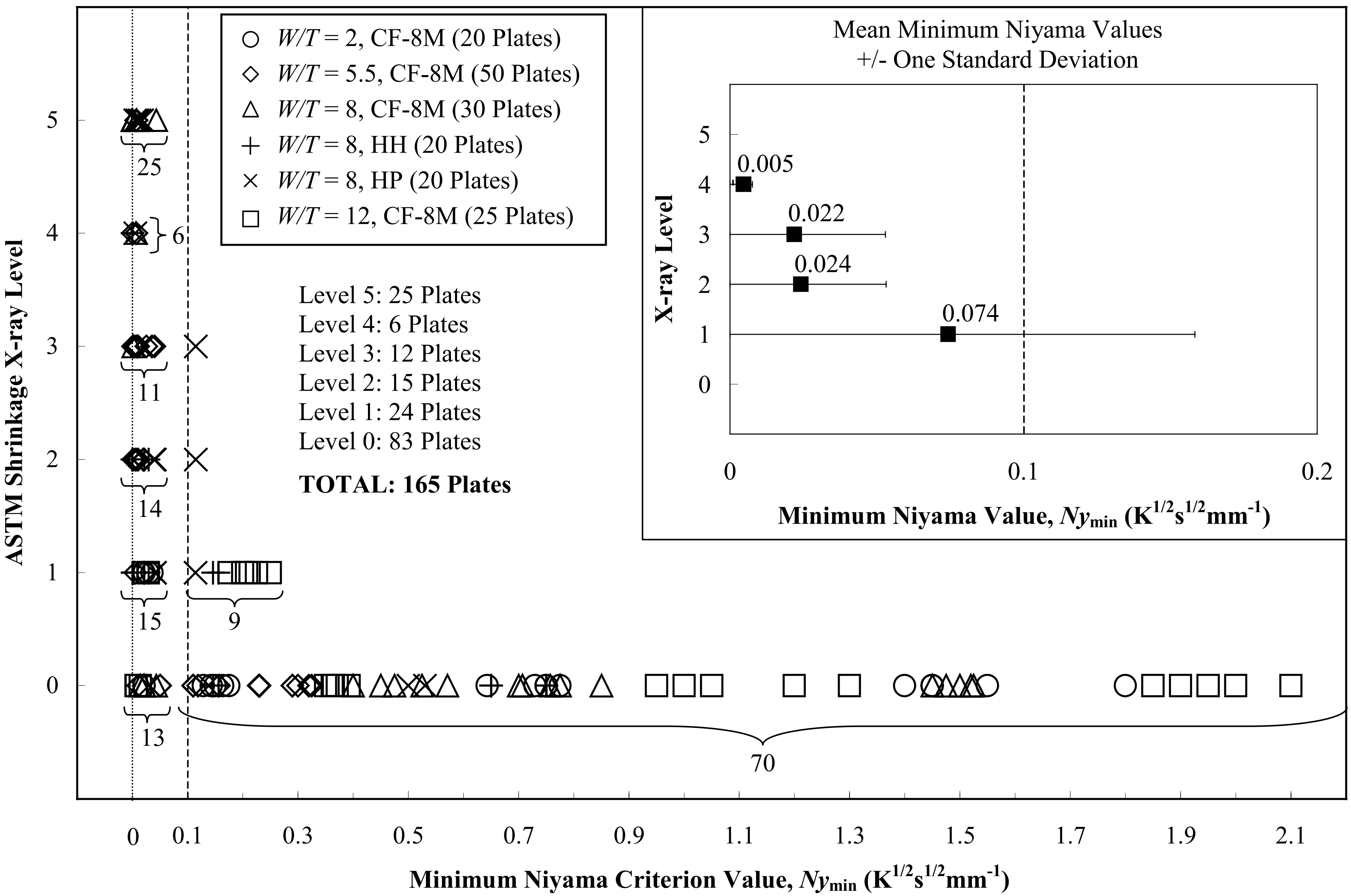

Figure 13 ASTM shrinkage x-ray level vs. minimum Niyama criterion value for the *W/T* = 2, 5.5, 8 and 12 plates.

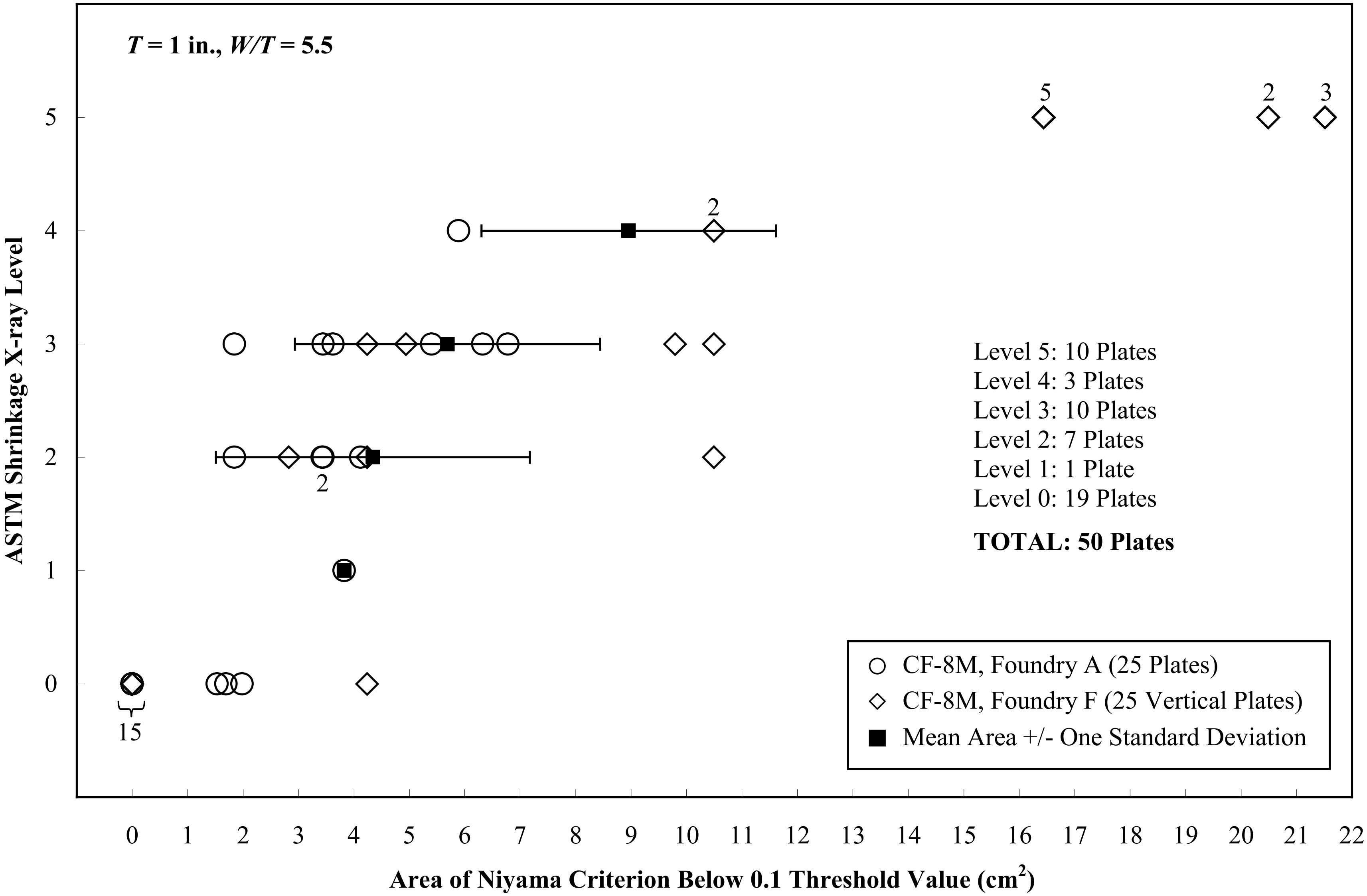

Figure 14 Casting soundness vs. area of cells below Niyama criterion threshold value of 0.1 $(K\,s)^{1/2}/mm$, for the W/T = 5.5 plates.

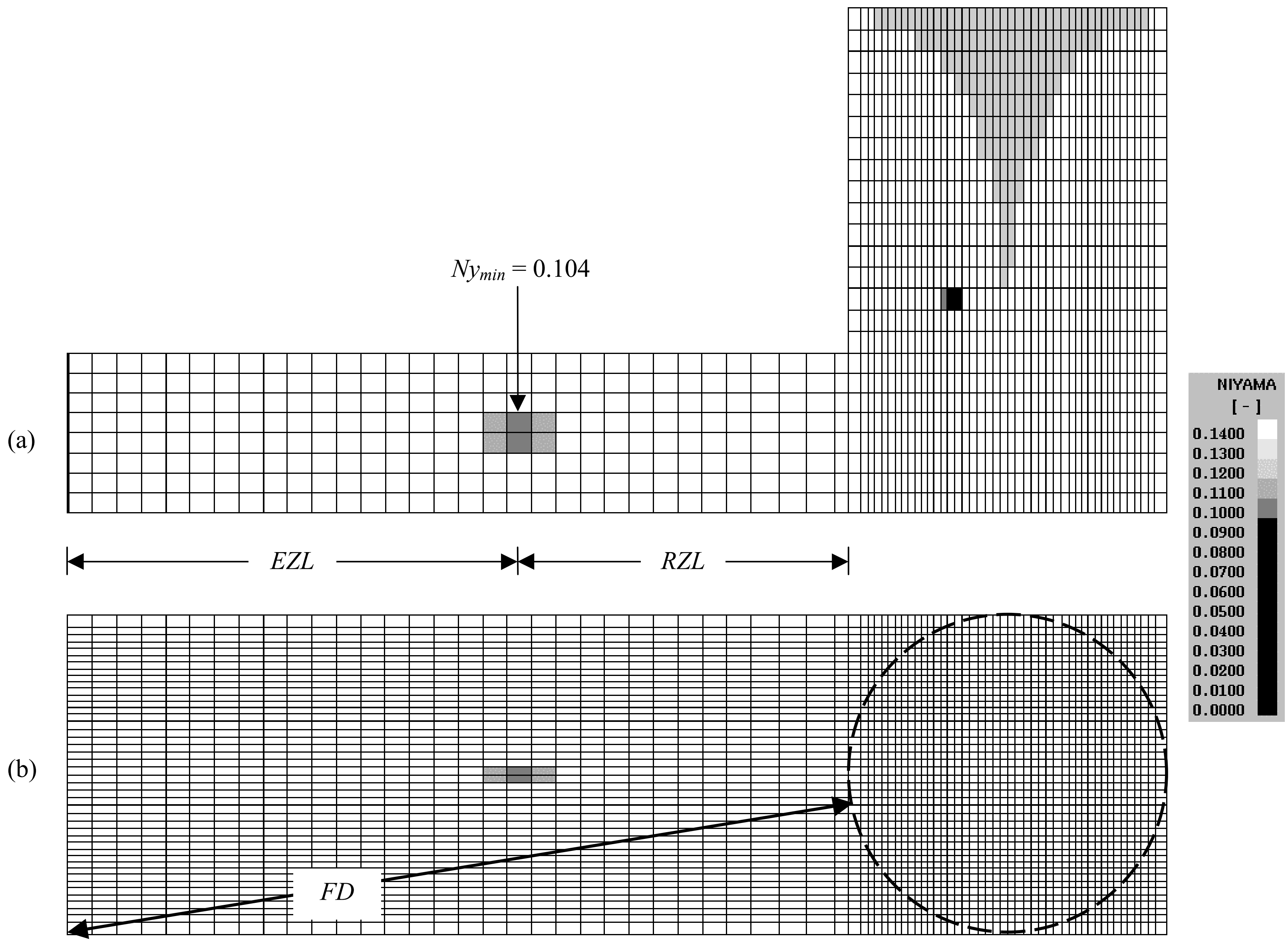

Figure 15 Cross-section side view (a) and top view (b) Niyama plots from a simulation of a 7.62 cm by 15.2 cm by 52.6 cm (3 in. *T* by 6 in. *W* by 20.7 in. *L*) top-risered AISI 1025 steel plate.

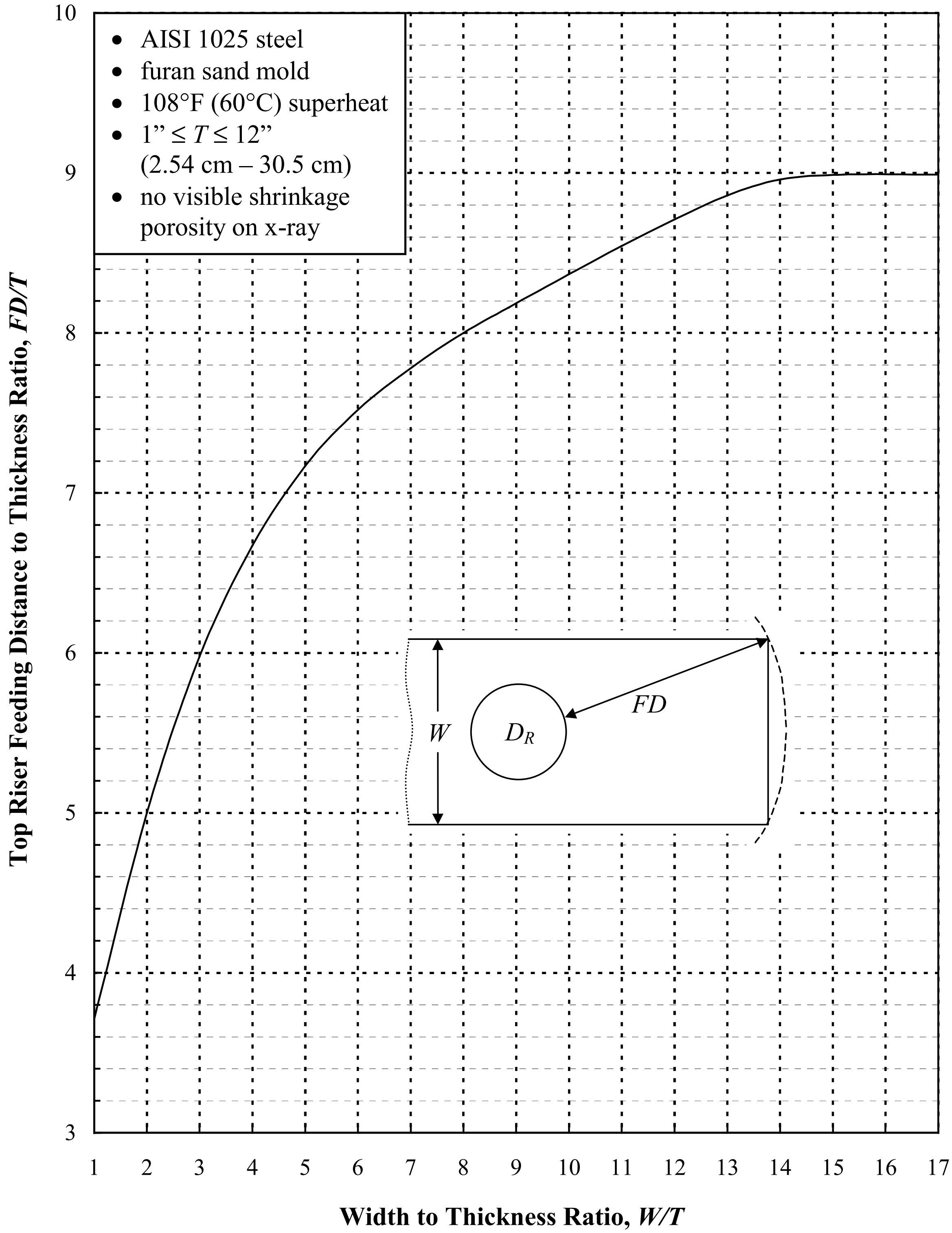

Figure 16 Feeding distance (*FD*) as a function of width and thickness for top-risered sections cast with plain carbon steel.

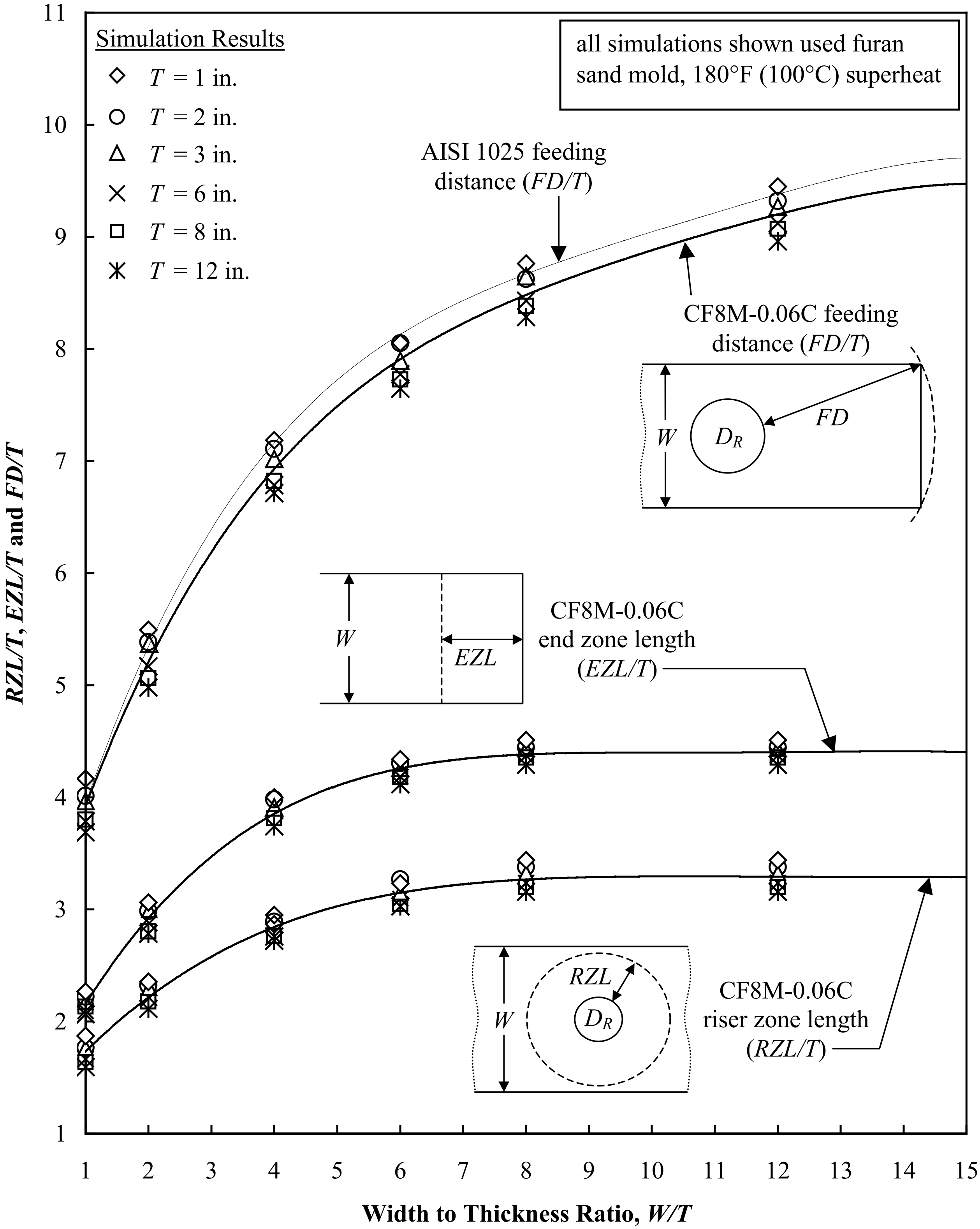

Figure 17 Riser zone length, end zone length and feeding distance curves for CF-8M (0.06 pct carbon), all normalized by the thickness T, shown with simulation results for various thicknesses.

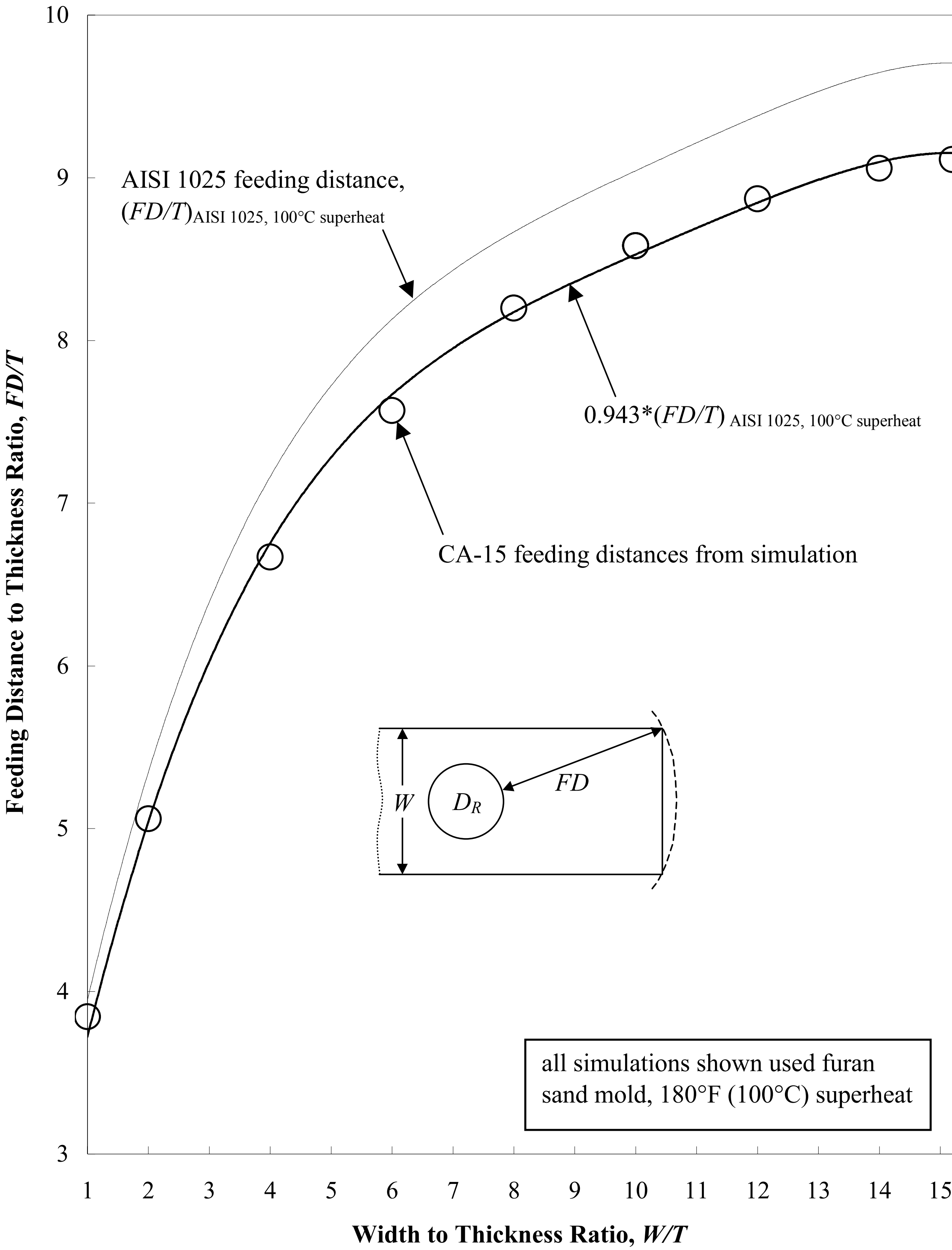

Figure 18 Feeding distance results for CA-15 (open circles), compared with AISI 1025 feeding distance curve, scaled by 0.943.

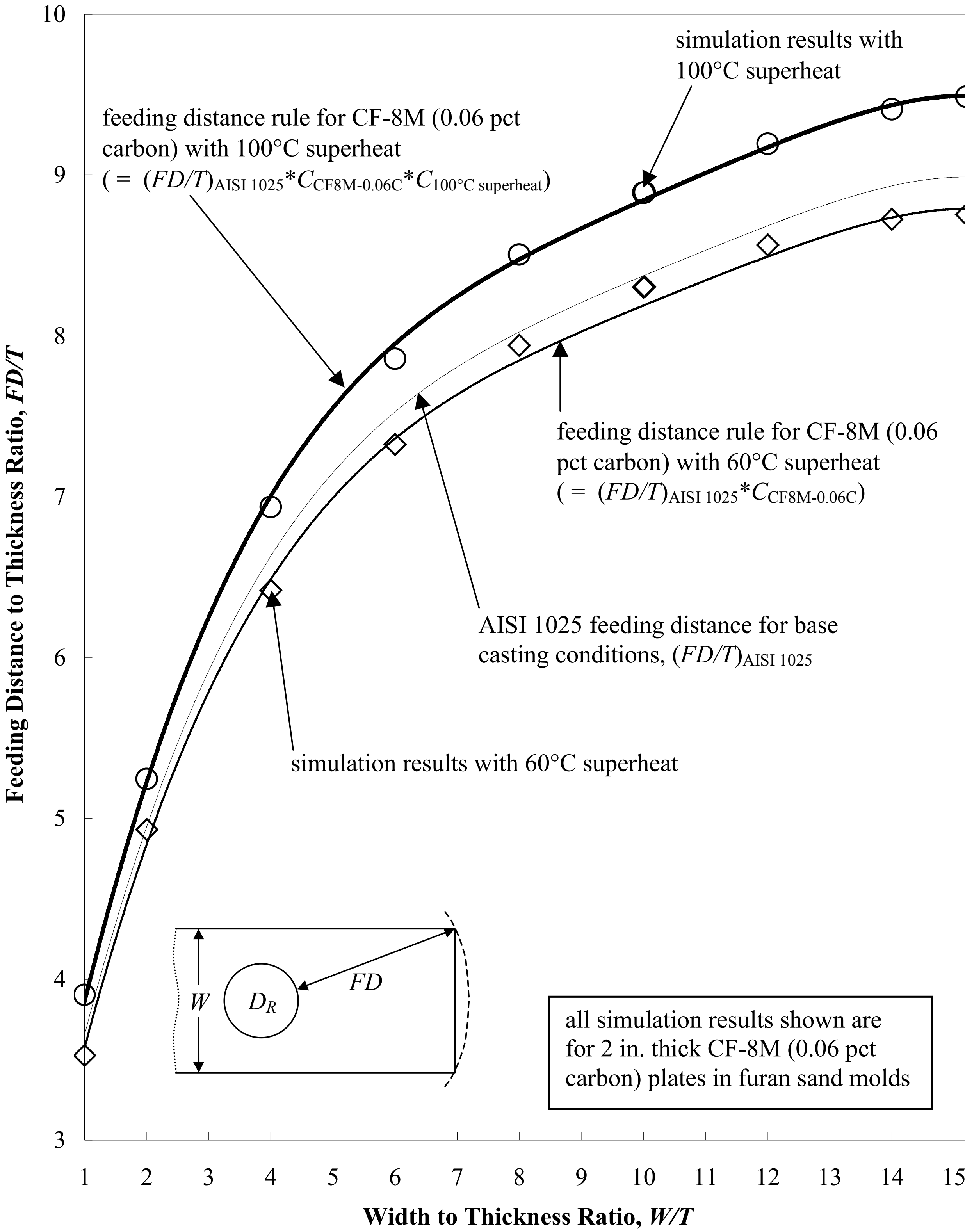

Figure 19 Comparison between CF-8M (0.06 pct carbon) simulation results and values calculated using feeding distance rule. (FD/T)AISI 1025 is calculated using Eq. (1); multipliers $C_{\text{CF8M-0.06C}}$ and $C_{100°\text{C superheat}}$ are from Table 1.

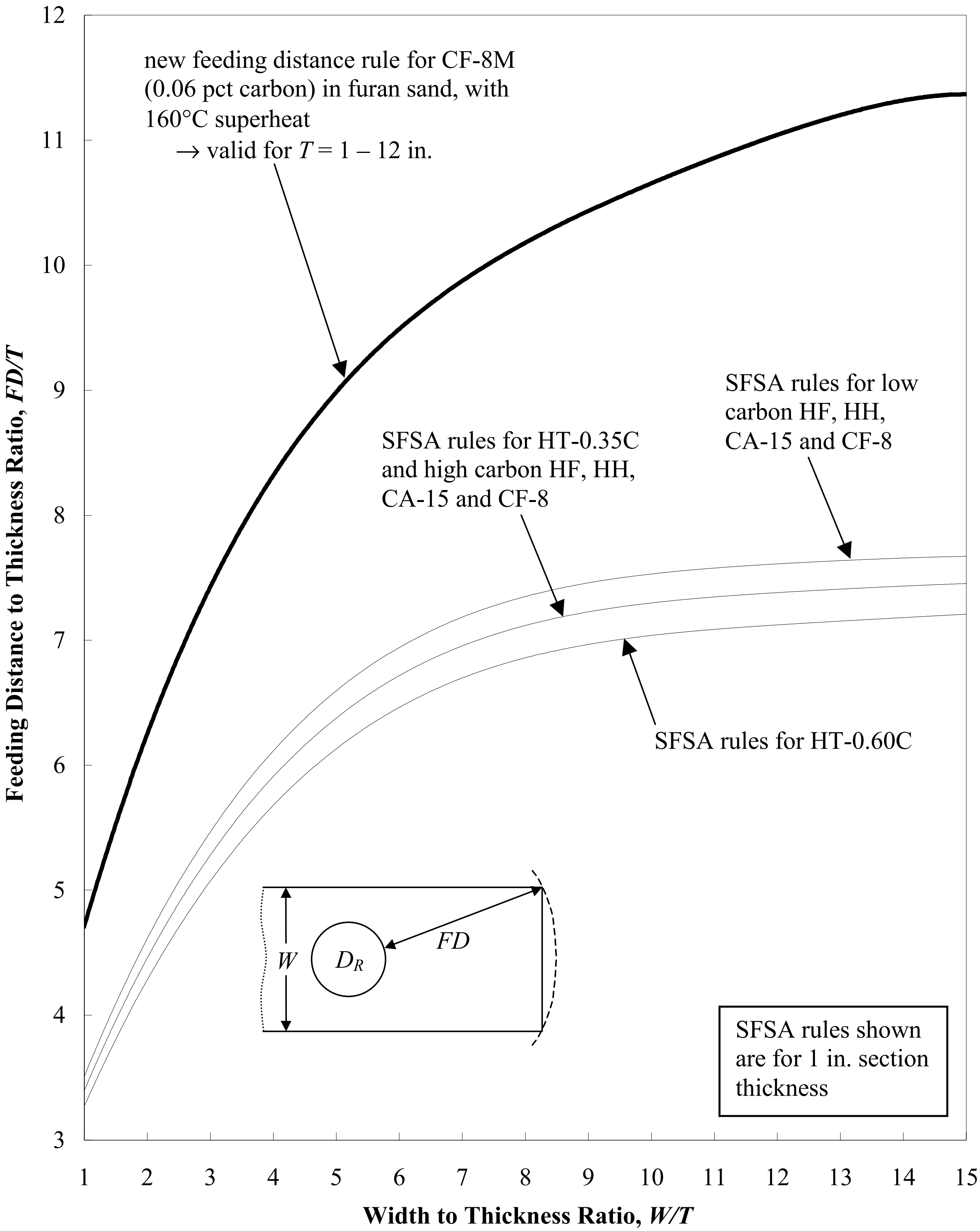

Figure 20 Comparison between existing rules[29] and the new feeding distance rule for CF-8M (0.06 pct carbon) in furan sand with a 160ºC superheat.

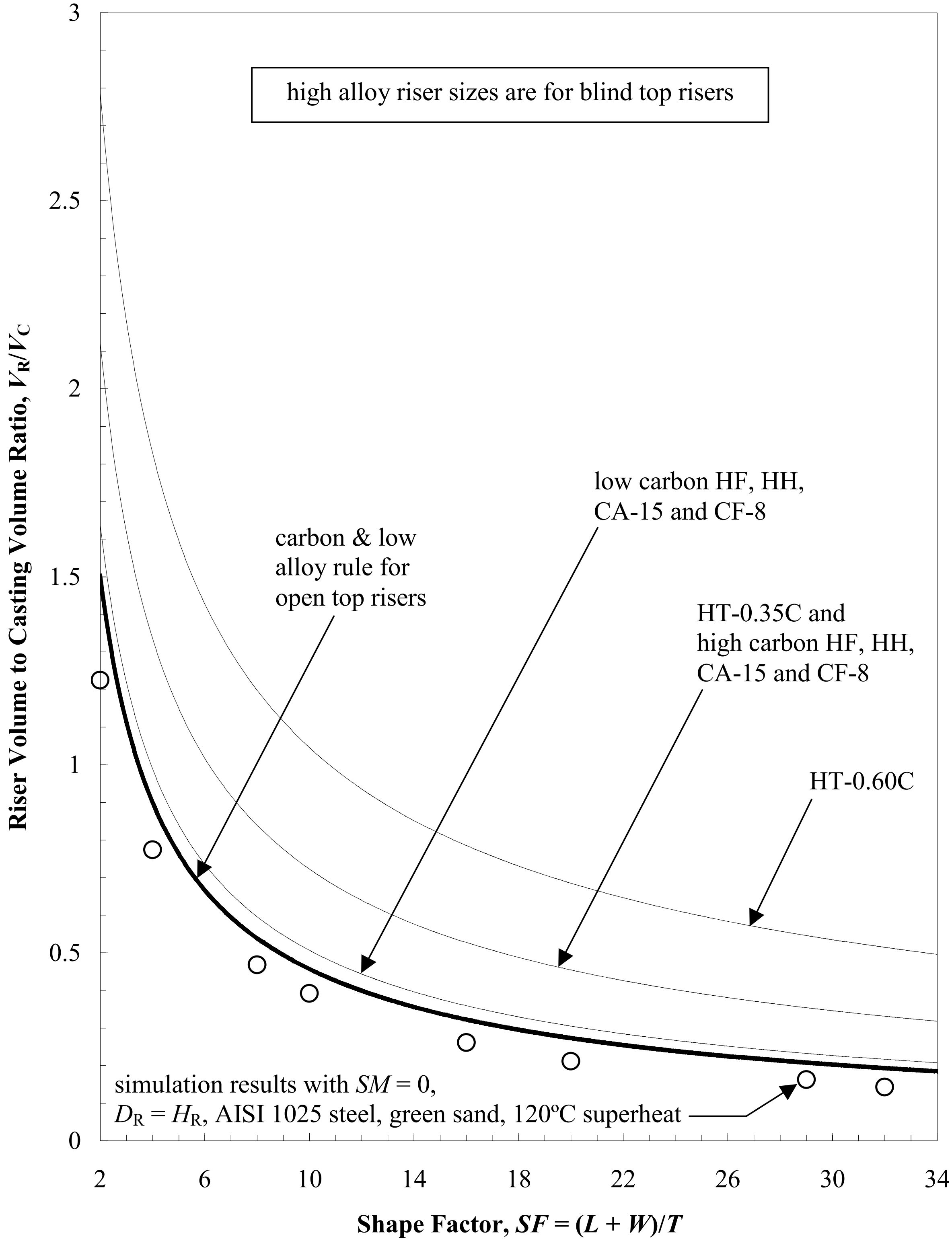

Figure 21 Direct comparison between the C&LA riser sizing rules of Bishop *et al*.[26] and the high alloy riser sizing rules of Varga *et al*.[17]

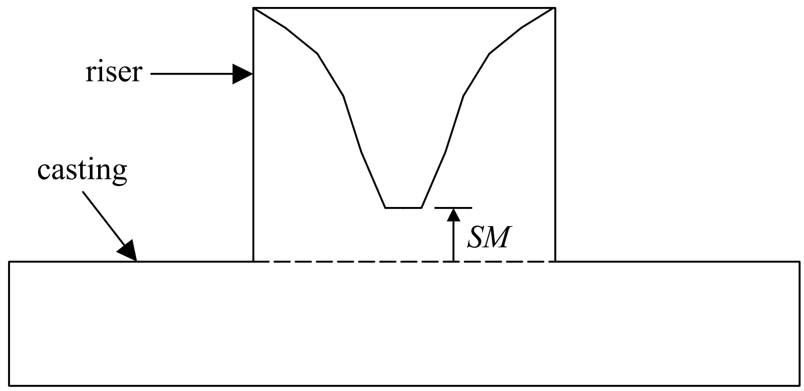

Figure 22 Sketch illustrating the definition of safety margin (*SM*).

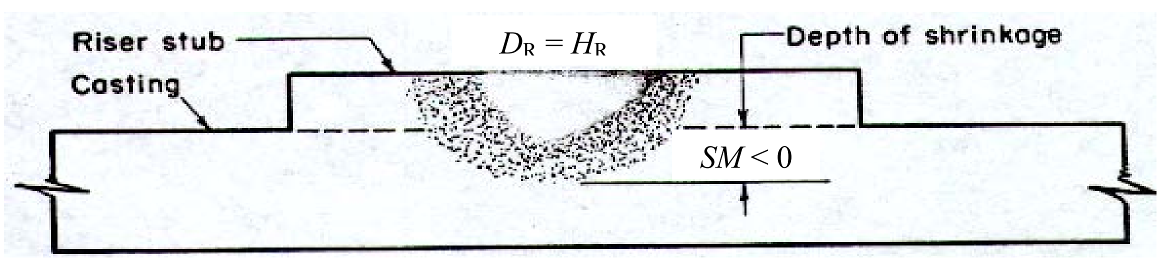

Figure 23 Illustration of negative safety margin (*SM*) due to insufficient riser size. Reproduced from Varga *et al*.[17]

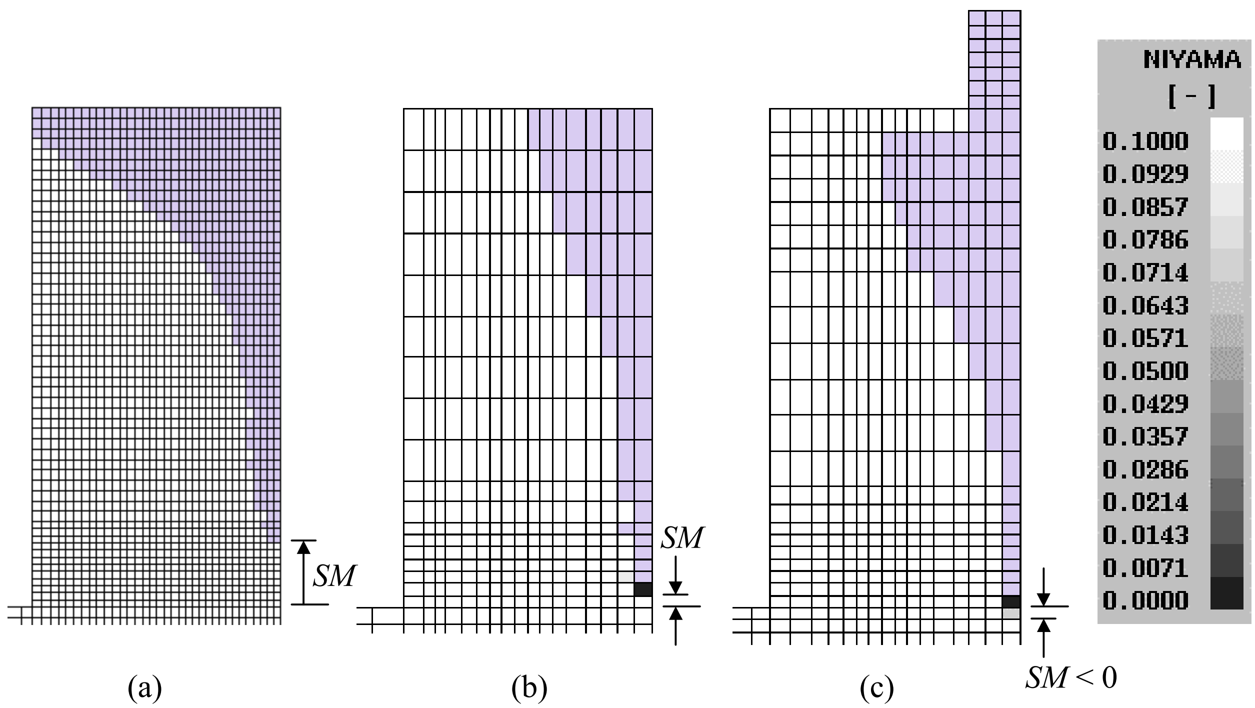

(a)
open top riser
SM = 0.41 in.

(b)
vented blind
top riser,
SM = 0.07 in.

(c)
blind top riser,
with cracker core
SM = -0.08 in.

Figure 24 Comparison of safety margins (*SM*) for a CA-15 plate casting with different types of risers.

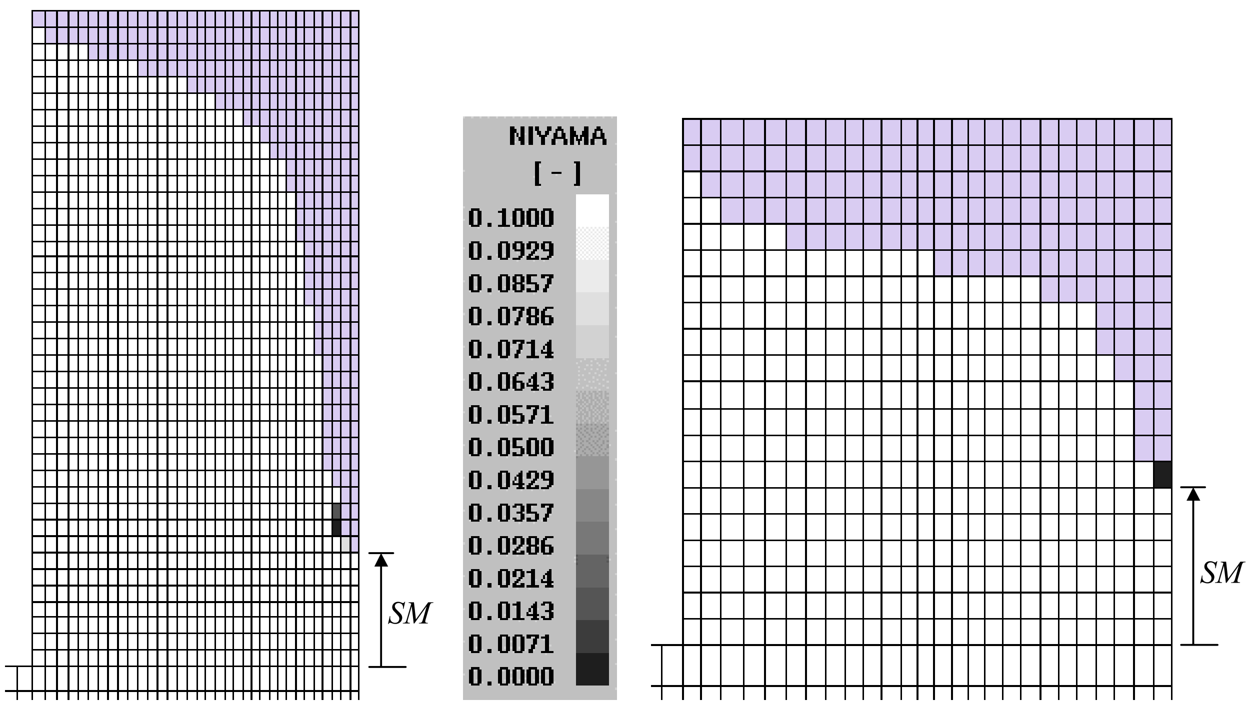

Casting: 4 x 4 x 12 in.
Riser: D_R = 6 in., H_R = 6 in.
Measured *SM* = 1.0 in.
Simulated *SM* = 1.1 in.

Casting: 2 x 36 x 36 in.
Riser: D_R = 12 in., H_R = 6.5 in.
Measured *SM* = 2.0 in.
Simulated *SM* = 1.97 in.

Figure 25 Comparison between simulated safety margins (*SM*) and measured values from Bishop *et al*.[26] for 1025 steel.

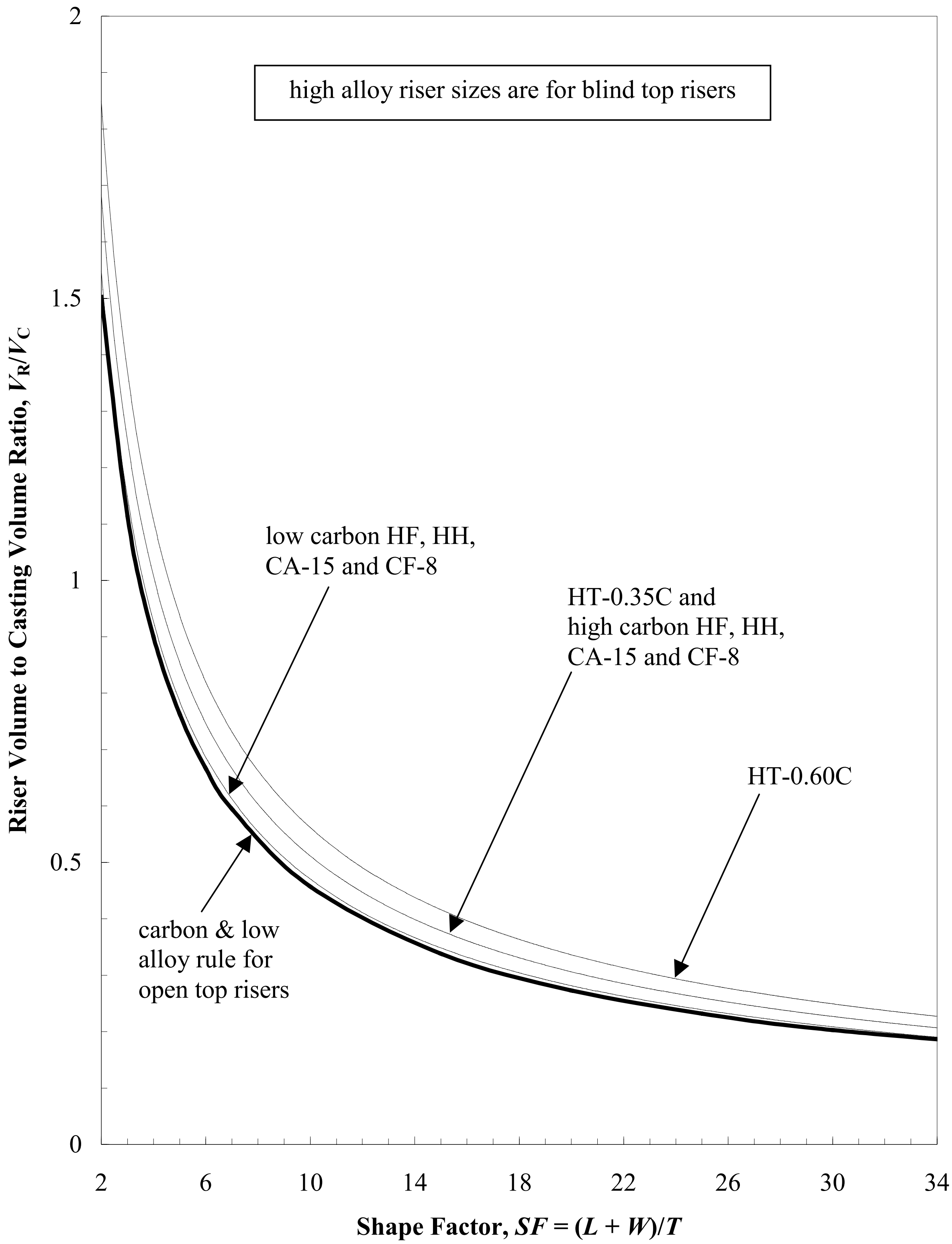

Figure 26 Comparison between the C&LA riser sizing rules of Bishop *et al*.[26] and the high alloy riser sizing rules of Varga *et al*,[17] if the high alloy rules are sized according to the methodology of Bishop *et al*.

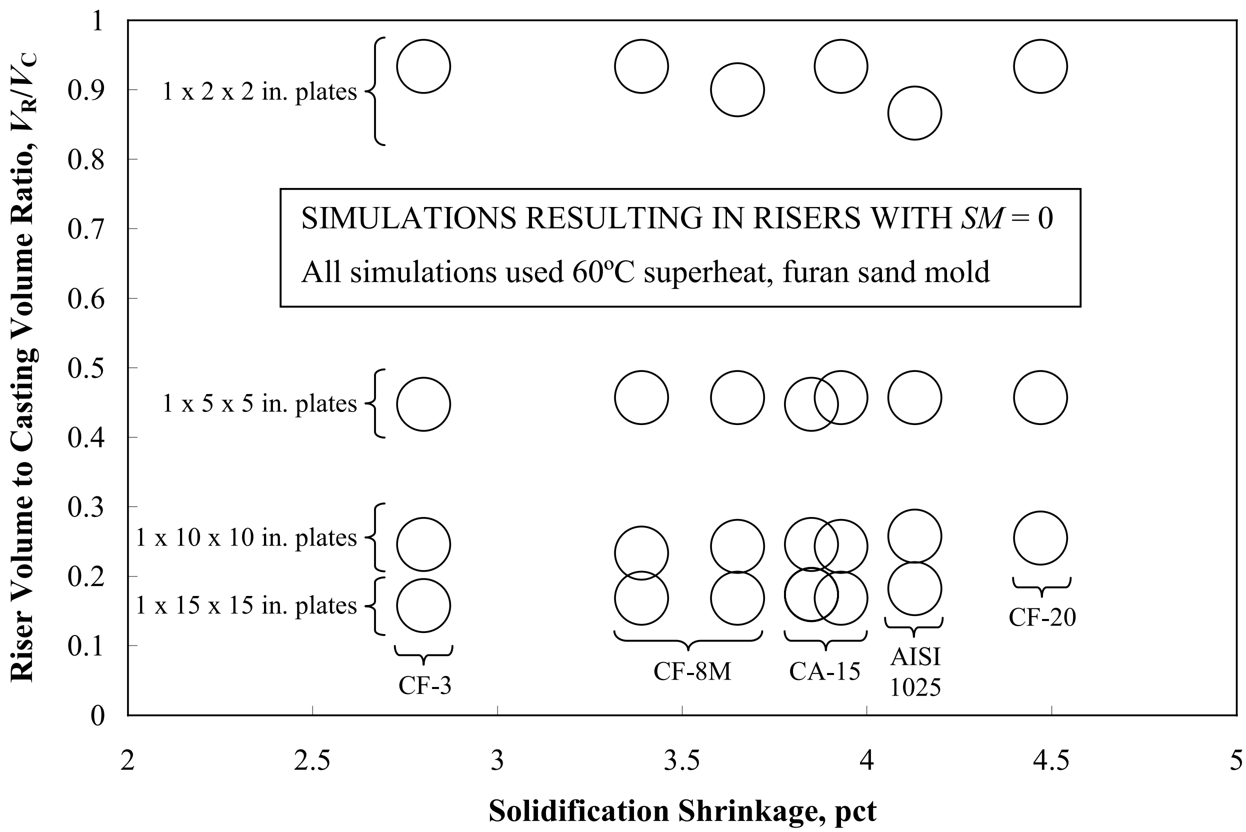

Figure 27 Minimum riser sizes (based on a safety margin of zero) for various alloys.

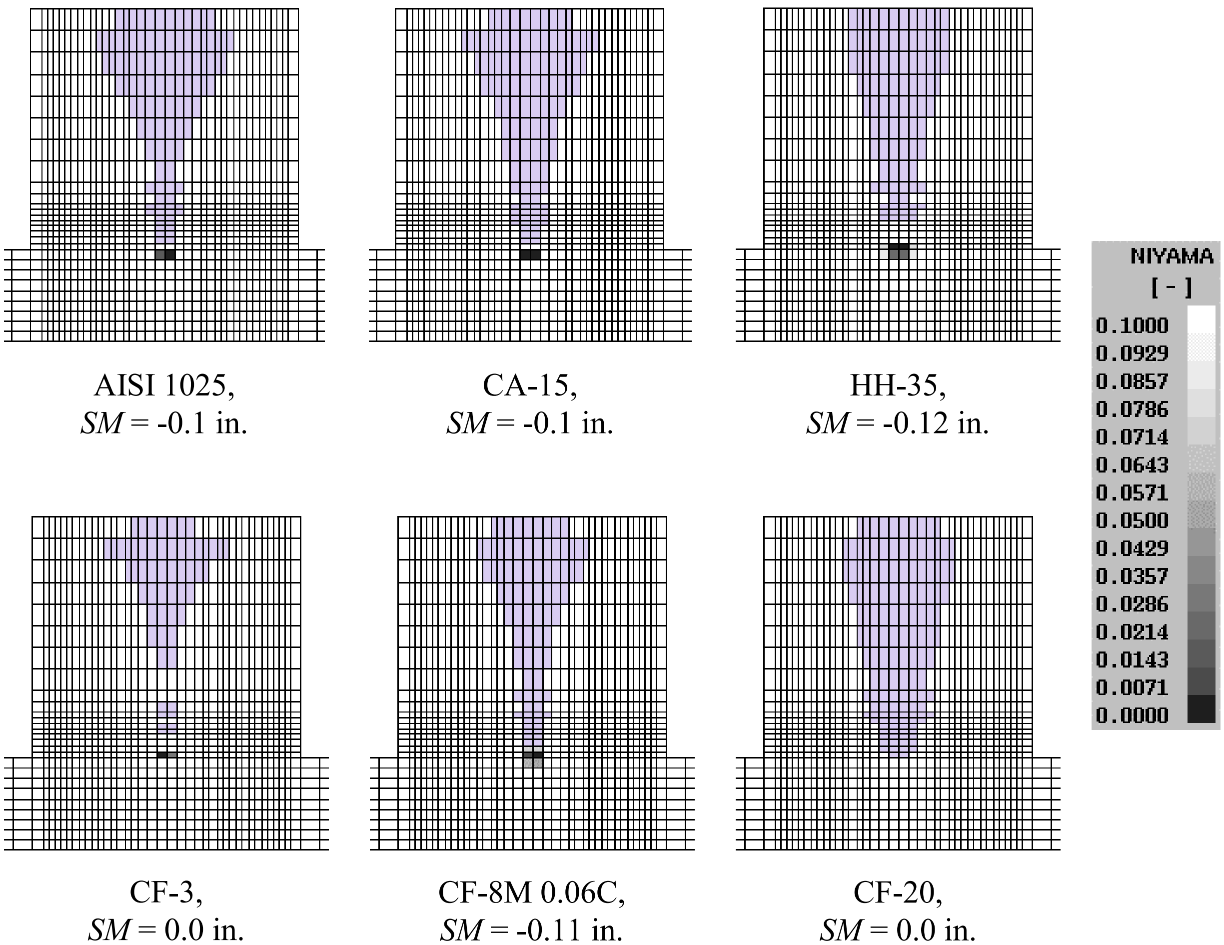

Figure 28 Comparison between riser pipes of different steel alloys. All risers shown are vented top blind risers.